Flexural Strength of Reinforced and Prestressed Concrete T-Beams

Stephen J. Seguirant, P.E.
Vice President and
Director of Engineering
Concrete Technology Corporation
Tacoma, Washington

Richard Brice, P.E.
Bridge Software Engineer
Bridge & Structures Office
Washington State Department of Transportation
Olympia, Washington

Bijan Khaleghi, Ph.D., P.E.
Concrete Specialist
Bridge & Structures Office
Washington State Department of Transportation
Olympia, Washington

The calculation of the flexural strength of concrete T-beams has been extensively discussed in recent issues of the PCI JOURNAL. The debate centers on when T-beam behavior is assumed to begin. The AASHTO LRFD Bridge Design Specifications (LRFD) maintain that it begins when c (distance from extreme compression fiber to neutral axis) exceeds the thickness of the flange. The AASHTO Standard Specifications for Highway Bridges (STD), and other references, contend that it begins when a (depth of equivalent rectangular stress block) exceeds the flange thickness. This paper examines the fundamentals of T-beam behavior at nominal flexural strength, and compares the results of LRFD and STD with more rigorous analyses, including the PCI Bridge Design Manual (PCI BDM) method and a strain compatibility approach using nonlinear concrete compressive stress distributions. For pretensioned T-beams of uniform strength, a method consisting of a mixture of LRFD and STD is investigated. For T-beams with different concrete strengths in the flange and web, the PCI BDM method is compared with the nonlinear strain compatibility analysis. High strength concretes (HSC) up to 15,000 psi (103 MPa) are considered. The selection of appropriate ϕ factors and maximum reinforcement limits is also discussed. Comparisons with previous tests of T-beams are presented, and revisions to the relevant sections of LRFD are proposed.

The proper calculation of the flexural strength of T-beams has been the subject of much discussion in recent issues of the PCI JOURNAL.[1-3] There is a distinct difference in the calculated capacities of reinforced and prestressed concrete T-beams determined by the AASHTO LRFD Bridge Design Specifications (LRFD),[4] and the methods given in other codes and references,[5-7] including the AASHTO Standard Specifications for Highway Bridges (STD).[8] The difference lies primarily in the treatment of the flange overhangs at nominal flexural strength.

References 5 through 8 claim that T-beam behavior begins when the depth of the equivalent rectangular compressive stress block, a, exceeds the thickness of the flange, h_f. Thus, the entire flange overhang area is allowed to carry a compressive stress of intensity $0.85f'_c$.

On the other hand, LRFD requires that a section be treated as a T-beam once the depth to the neutral axis, c, becomes greater than the thickness of the flange. The depth of the equivalent rectangular compressive stress block in the flange overhangs is limited to $a = \beta_1 h_f$, where the value of β_1 is between 0.65 and 0.85, depending on the strength of the concrete in the flange. Thus, the flange overhang area that is effective in resisting compression is reduced by between 15 and 35 percent when compared to other codes and references.

To ensure that equilibrium is maintained with the tension force in the steel, the loss of effective compressive area in the flange overhangs must be replaced by additional compressive area in the web. This results in a significant increase in the calculated depth to the neutral axis. The internal moment arm between the compression and tension forces is reduced, as is the calculated moment capacity.

This paper examines the behavior of T-beams at nominal flexural strength. The fundamental theory is explained, and equations are derived for the various calculation methods used in the study. Explanations are provided for the differences between the various methods, with special emphasis on the difference between the LRFD method and the methods of other codes and references.

Parametric studies are used to compare the results of the various calculation methods. For non-prestressed T-beams, the LRFD and STD methods are compared with the results of a strain compatibility analysis using nonlinear concrete compressive stress-strain curves. The nonlinear analysis removes β_1 as a variable, and allows for a fair comparison between the three calculation methods. Concrete strengths ranging from 7000 to 15,000 psi (48.3 to 103 MPa) are investigated.

Prestressed beams are also evaluated. In one study, the flexural strength of pretensioned T-beams with a concrete strength of 7000 psi (48.3 MPa) in both the flange and web are compared using five different analyses: LRFD, STD, the PCI Bridge Design Manual[9] (PCI BDM) strain compatibility method, a nonlinear strain compatibility analysis, and an analysis mixing the LRFD and STD methods. In this case, the width of the flange is varied between 48 and 75 in. (1220 to 1905 mm) in 9 in. (229 mm) increments to determine the effect of flange width on the calculations.

Another study examines pretensioned beams with concrete strengths ranging from 7000 to 15,000 psi (48.3 to 103 MPa) in the web and 4000 to 8000 psi (27.6 to 55.2 MPa) in the flange. Since the LRFD and STD methods are not adaptable to this analysis, only the PCI BDM and nonlinear strain compatibility methods will be compared. This comparison is used to evaluate the average β_1 approach of the PCI BDM method.

The increase in the calculated depth to the neutral axis resulting from LRFD impacts the design of T-beams in other ways than simply reducing the design flexural strength. Since LRFD limits the effectiveness of the tension reinforcement to beams with c/d_e ratios less than or equal to 0.42, an increase in c will lead to beams with reduced maximum reinforcement ratios. Thus, beams become over-reinforced more quickly using LRFD than other codes and references.

For under-reinforced members, the resistance factor ϕ is taken as 0.9 for non-prestressed flexural members and 1.0 for precast, prestressed flexural members in both LRFD and STD. Neither specification allows over-reinforced non-prestressed flexural members. However, both specifications allow over-reinforced prestressed flexural members, but no credit is given for reinforcement in excess of that which would result in an under-reinforced section.

LRFD allows over-reinforced prestressed and partially prestressed members if "it is shown by analysis and experimentation that sufficient ductility of the structure can be achieved." No guidance is given for what "sufficient ductility" should be, and it is not clear in either specification what value of ϕ should be used for such over-reinforced members, though some designers have used $\phi = 0.7$.[2] Maximum reinforcement limits and appropriate resistance factors will both be discussed with respect to prestressed and non-prestressed flexural members.

To validate the analysis procedures, available test data are evaluated and compared with the results of the various calculation methods. Recommended revisions to LRFD are also presented.

THEORETICAL CONSIDERATIONS

Assumptions

The following assumptions are adapted from Reference 10, and are common to all of the calculation methods used in this study, except as noted:

1. The strength design of flexural members is based on satisfaction of applicable conditions of equilibrium and compatibility of strains.
2. Strain in bonded reinforcement and concrete is assumed to be directly proportional to the distance from the neutral axis.
3. The maximum usable strain at the extreme concrete compression fiber is assumed to be 0.003.
4. For non-prestressed reinforcement, stress in the reinforcement below the specified yield strength f_y for the grade of reinforcement used is taken as E_s times the steel strain. For strains greater than that corresponding to f_y, stress in the reinforcement is considered independent of strain and is equal to f_y. For prestressing steel, f_{ps} is substituted for f_y in strength computations.

5. The tensile strength of concrete is neglected in all flexural strength calculations.
6. The relationship between the concrete compressive stress distribution and concrete strain is assumed to be rectangular for all calculation methods of this paper except the nonlinear analysis. For this analysis, the nonlinear concrete stress-strain relationship is taken from Collins and Mitchell.[11]
7. For the equivalent rectangular concrete stress distribution, the following assumptions are made:
   - A concrete stress of $0.85f'_c$ is assumed to be uniformly distributed over an equivalent compression zone bounded by the edges of the cross section and a straight line located parallel to the neutral axis at a distance $a = \beta_1 c$ from the fiber of maximum compressive strain. An exception to this is the flange overhangs in the LRFD method, where the compression zone is limited to the upper $\beta_1 h_f$ of the flange.
   - The distance c from the fiber of maximum compressive strain to the neutral axis is measured in a direction perpendicular to that axis.
   - The value of β_1 is taken as 0.85 for concrete strengths f'_c up to and including 4000 psi (27.6 MPa). For strengths above 4000 psi (27.6 MPa), β_1 is reduced continuously at a rate of 0.05 for each 1000 psi (6.9 MPa) of strength in excess of 4000 psi (27.6 MPa), but β_1 is not taken less than 0.65.

For composite sections, the prestress applied to the beam combined with the dead load of the beam and wet concrete in the deck will cause a strain discontinuity at the interface between the beam and deck. Over time, these stresses redistribute between the beam and deck due to differential shrinkage and creep. This discontinuity has traditionally been ignored in the calculation of the flexural strength of the composite member, and will also be ignored in the parametric studies of this paper.

Derivation of Equations for the Flexural Strength of T-Beams

Although the parametric studies do not include mild steel compression reinforcement, and the studies of prestressed concrete members do not include mild steel tension reinforcement, the following derivations for LRFD and STD include both for the sake of completeness. Note that whenever mild steel compression reinforcement is considered in the calculations, the stress should be checked to ensure that the compression steel has yielded. If not, the stress in the steel determined by strain compatibility should be used.

The analysis of prestressed concrete members is complicated by the nonlinear stress-strain behavior of the prestressing steel. In non-prestressed concrete members, the stress in the steel is defined by the bilinear relationship described in Assumption No. 4 above. This is not the case with prestressing steel, and the stress in the steel at nominal strength, f_{ps}, must be estimated in order to determine the flexural strength of the beam. This is handled in different ways in the derivations below.

For consistency, the notation used in the derivations is that of LRFD wherever possible.

AASHTO LRFD Equations

The derivation[12] of the equations in LRFD begins with an estimate of the stress in the prestressing steel at nominal flexural strength:

$$f_{ps} = f_{pu}\left(1 - k\frac{c}{d_p}\right) \tag{1}$$

for which:

$$k = 2\left(1.04 - \frac{f_{py}}{f_{pu}}\right) \tag{2}$$

Fig. 1 shows a schematic of the condition of the T-beam at nominal flexural strength. Since LRFD requires that the beam be treated as a T-beam once c exceeds h_f, the depth of the equivalent rectangular compressive stress block in the flange overhangs is limited to $\beta_1 h_f$. In order for equilibrium to be maintained:

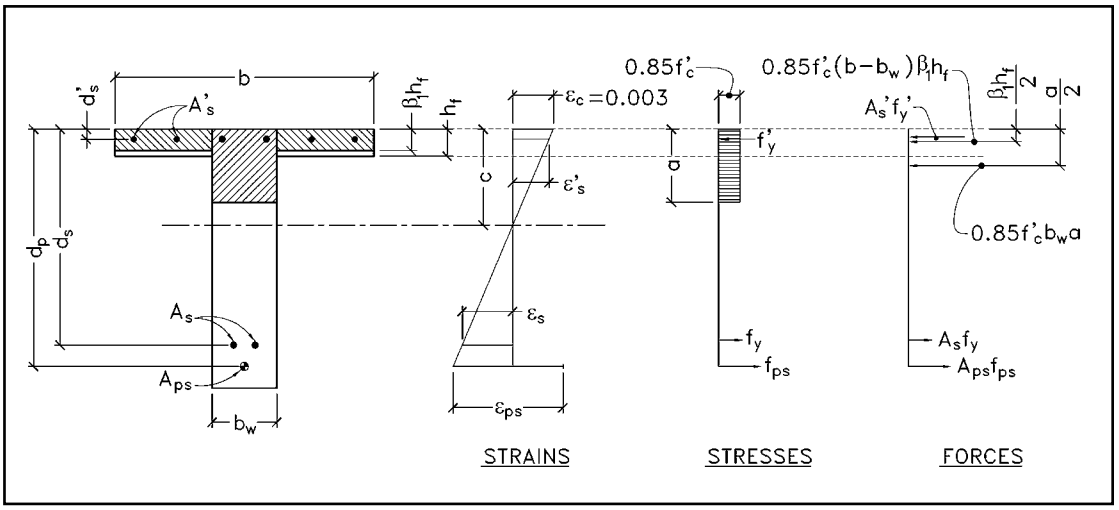

Fig. 1. AASHTO LRFD T-beam flexural strength computation model.

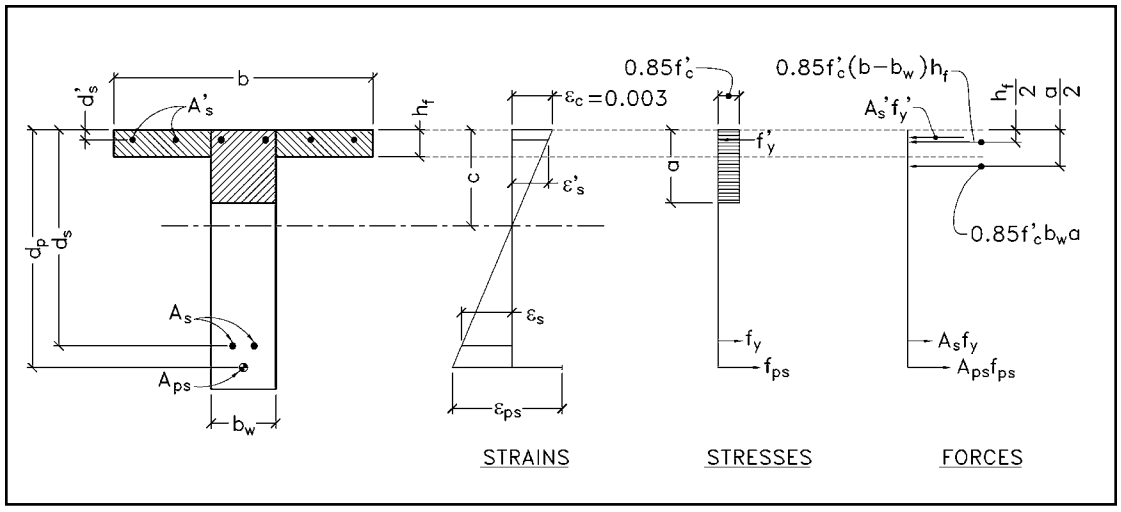

Fig. 2. AASHTO STD T-beam flexural strength computation model.

$$A_{ps}f_{ps} + A_s f_y - A'_s f'_y = 0.85f'_c\, b_w \beta_1 c + 0.85f'_c\,(b - b_w)\,\beta_1 h_f \quad (3)$$

Substituting Eq. (1) into Eq. (3) for f_{ps}:

$$A_{ps}f_{pu} - A_{ps}f_{pu}\,k\,\frac{c}{d_p} + A_s f_y - A'_s f'_y = 0.85f'_c\, b_w \beta_1 c + 0.85f'_c\,(b - b_w)\,\beta_1 h_f \quad (4)$$

Moving terms including c to the right-hand side of the equation:

$$A_{ps}f_{pu} + A_s f_y - A'_s f'_y - 0.85f'_c\,(b - b_w)\,\beta_1 h_f = 0.85f'_c\, b_w \beta_1 c + kA_{ps}\,\frac{f_{pu}}{d_p}\,c \quad (5)$$

Solving for c:

$$c = \frac{A_{ps}f_{pu} + A_s f_y - A'_s f'_y - 0.85f'_c\,(b - b_w)\,\beta_1 h_f}{0.85f'_c\, b_w \beta_1 + kA_{ps}\,\frac{f_{pu}}{d_p}} \quad (6)$$

This equation is LRFD Eq. 5.7.3.1.1-3. The moment capacity is then calculated by summing the moments about the centroid of the compression force in the web:

$$M_n = A_{ps}f_{ps}\left(d_p - \frac{a}{2}\right) + A_s f_y\left(d_s - \frac{a}{2}\right) - A'_s f'_y\left(d'_s - \frac{a}{2}\right) + 0.85f'_c\,(b - b_w)\,\beta_1 h_f\left(\frac{a}{2} - \frac{\beta_1 h_f}{2}\right) \quad (7)$$

Note that the very last term of Eq. (7) includes a β_1 factor that is not included in LRFD Eq. 5.7.3.2.2-1. This β_1 factor is necessary to obtain the proper moment arm between the compression force in the web and the compression force in the reduced area of the flange overhangs. Eqs. (1), (2), (6) and (7) are used in the parametric studies.

AASHTO STD Equations

The equations for the flexural strength of T-beams in STD[8] appear to have been derived from ACI 318R-83,[6] which in turn were derived from Mattock et al.[5] These references use different notation and formats for the equations, but they are all derived from the same model, shown in Fig. 2. None of the equations in these references include mild steel reinforcement in the compression zone.

The only difference between the models of Figs. 1 and 2 is the treatment of the flange overhangs. In Fig. 2, the entire area of the flange overhangs is covered with a compressive stress of intensity $0.85f'_c$. In order to be consistent with LRFD, the same notation and sequence will be used in the derivation below, and mild steel compression reinforcement will be included. For equilibrium of forces in Fig. 2:

$$A_{ps}f_{ps} + A_s f_y - A'_s f'_y = 0.85f'_c\, b_w \beta_1 c + 0.85f'_c\,(b - b_w)\,h_f \quad (8)$$

Solving for a:

$$a = \beta_1 c = \frac{A_{ps}f_{ps} + A_s f_y - A'_s f'_y - 0.85f'_c\,(b - b_w)\,h_f}{0.85f'_c\, b_w} \quad (9)$$

Summing the moments about the centroid of the compression force in the web:

$$M_n = A_{ps}f_{ps}\left(d_p - \frac{a}{2}\right) + A_s f_y\left(d_s - \frac{a}{2}\right) - A'_s f'_y\left(d'_s - \frac{a}{2}\right) + 0.85f'_c\,(b - b_w)\,h_f\left(\frac{a}{2} - \frac{h_f}{2}\right) \quad (10)$$

Eq. (10) appears to be significantly different from Eq. 9-14a of STD, which is expressed as:

$$\phi M_n = \phi\left[A_{sr}f_{su}^{*}\,d\left(1 - 0.6\,\frac{A_{sr}f_{su}^{*}}{b'df'_c}\right) + A_s f_{sy}\,(d_t - d) + 0.85f'_c\,(b - b')t(d - 0.5t)\right] \quad (11)$$

where:

$$A_{sr} = A_s^{*} + \frac{A_s f_{sy}}{f_{su}^{*}} - A_{sf} \quad (12)$$

$$A_{sf} = \frac{0.85f'_c\,(b - b')t}{f_{su}^{*}} \quad (13)$$

However, algebraic manipulation shows that Eqs. (10) and (11) are in fact the same, although Eq. (11) does not include compression reinforcement. This derivation is shown in Appendix D of this paper, where Eq. (D-3) is the same as Eq. (10) except for the term representing mild steel compression reinforcement. The authors prefer the format of Eq. (10)

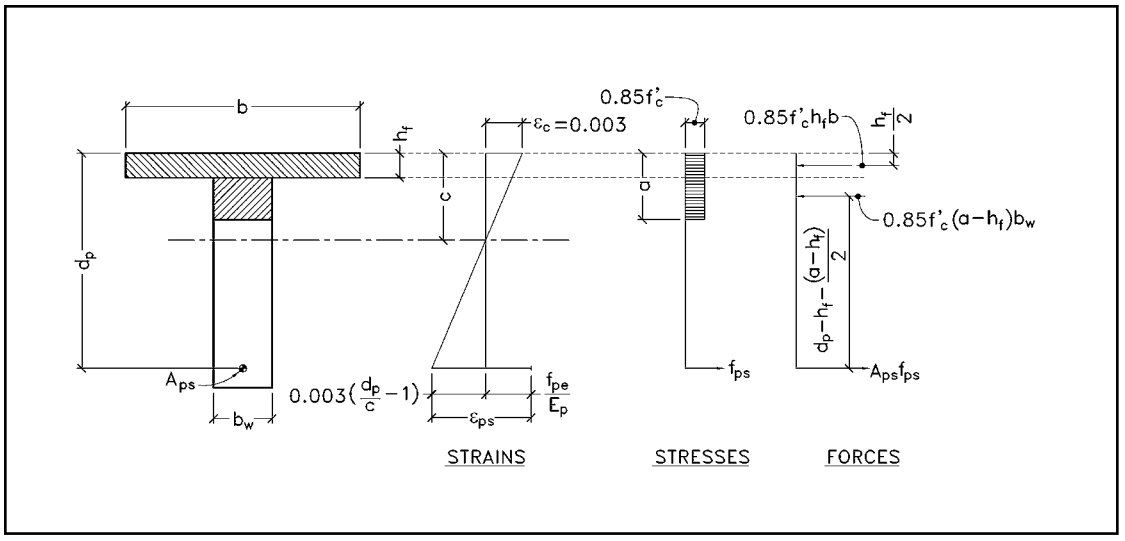

Fig. 3. PCI BDM T-beam flexural strength computation model.

to the format of STD because it is more transparent in its origin when considered in conjunction with Fig. 2. Eqs. (9) and (10) are used in the parametric studies.

All of the variables in Eq. (10) are known except for the stress in the prestressing steel at nominal flexural strength. Again, the value of f_{ps} must be estimated. STD provides the following equation for estimating the steel stress at nominal flexural strength (shown in LRFD notation):

$$f_{ps} = f_{pu}\left\{1 - \frac{k}{\beta_1}\left[\frac{A_{ps}f_{pu}}{bd_p f'_c} + \frac{d_s}{d_p}\left(\frac{A_s f_y}{bd_s f'_c}\right)\right]\right\} \quad (14)$$

For T-beams, this equation has been shown to slightly overestimate the value of f_{ps}.[1] The value of f_{ps} can be more accurately determined by strain compatibility, as will be seen in the parametric studies. Eq. (14) is used in the parametric studies for comparison purposes.

PCI Bridge Design Manual Strain Compatibility Analysis

The PCI BDM strain compatibility analysis is an iterative process where a value for the depth to the neutral axis is chosen and, based on a maximum concrete strain of 0.003 at the extreme compression fiber of the beam, the strains and corresponding stresses are calculated in both the concrete and each layer of bonded steel. The resulting forces must be in equilibrium, or another value of c must be chosen and the process repeated.

A schematic of the condition of the T-beam at nominal flexural strength for this method is shown in Fig. 3. Since no mild steel reinforcement is used in the parametric studies performed with this method, none is shown in Fig. 3, or in the derivations that follow. The PCI BDM provides a more generalized presentation of this method.

Based on the assumed value of c, the strain in the prestressing steel is calculated by:

$$\varepsilon_{ps} = 0.003\left(\frac{d_p}{c} - 1\right) + \frac{f_{pe}}{E_p} \quad (15)$$

The effective prestress, f_{pe}, is estimated in the parametric studies to be 158 ksi (1090 MPa) for beams with 20 strands, and is adjusted linearly by 0.2 ksi (1.38 MPa) per strand above or below this value. The calculations are not particularly sensitive to the value of f_{pe}. The stress in the prestressing steel during each iteration is then determined by the calculated strain using the "power formula:"[24]

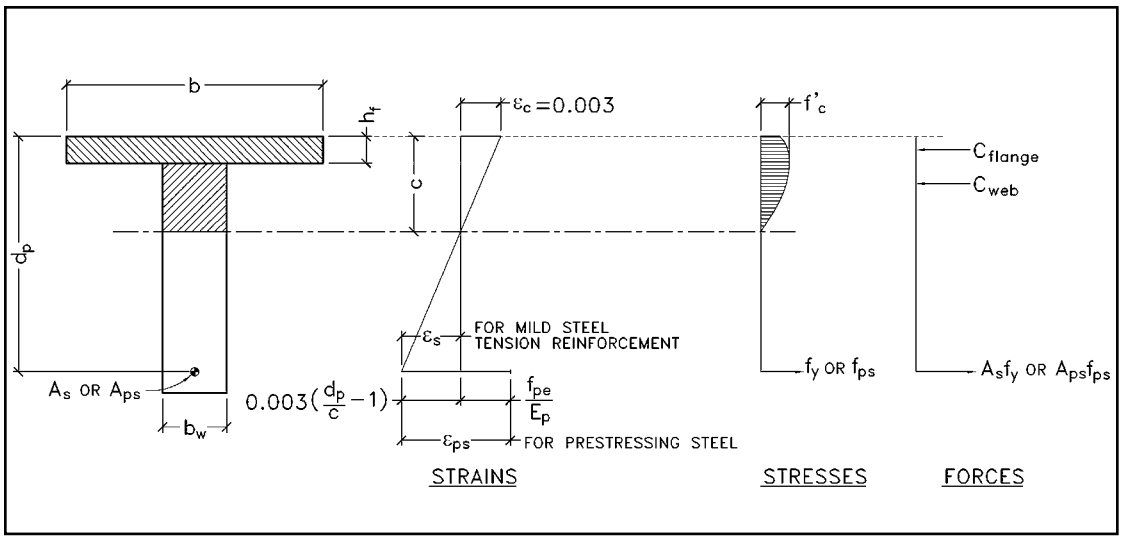

Fig. 4. Nonlinear T-beam flexural strength computation model.

$$f_{ps} = \varepsilon_{ps}\left[887 + \frac{27{,}613}{\left(1 + (112.4\varepsilon_{ps})^{7.36}\right)^{1/7.36}}\right] \leq 270 \text{ ksi (1862 MPa)} \quad (16)$$

The force in the steel can then be determined by:

$$\sum A_{si} f_{si} = A_{ps} f_{ps} \quad (17)$$

The assumptions associated with the equivalent rectangular concrete compressive stress distribution are the same as in STD, with one small exception. For simplicity of calculations, the STD derivation separates the flange overhangs from the web, and the web extends to the top of the member. Since the PCI BDM method may also apply to T-beams with different concrete strengths in the flange and web, the web is assumed to extend only to the bottom of the flange.

For T-beams of uniform concrete strength, the depth of the equivalent rectangular concrete compressive stress block can be calculated using the assumed depth to the neutral axis:

$$a = \beta_1 c \quad (18)$$

The compression forces are then:

$$\sum F_{cj} = 0.85 f'_c\, h_f b + 0.85 f'_c\, (a - h_f)\, b_w \quad (19)$$

Once the compression and tension forces are equalized, the sum of the moments about the prestressing steel results in the moment capacity:

$$M_n = 0.85 f'_c\, h_f b \left(d_p - \frac{h_f}{2}\right) + 0.85 f'_c\, (a - h_f)\, b_w \left(d_p - h_f - \frac{a - h_f}{2}\right) \quad (20)$$

In the case where the flange and web have different concrete strengths, the PCI BDM method uses an area-weighted value of β_1 given by:

$$\beta_{1(ave)} = \sum_j (f'_c A_c \beta_1)_j \Big/ \sum_j (f'_c A_c)_j \quad (21)$$

where A_c is the area of concrete in the flange or web.

Since the area of concrete in the web is a function of a, which in turn is a function of $\beta_{1(ave)}$, the value of $\beta_{1(ave)}$ must be assumed to calculate a, then checked with Eq. (21). Once the appropriate value of $\beta_{1(ave)}$ is determined, the compression forces can be calculated from:

$$\sum F_{cj} = 0.85 f'_{c\,(flange)}\, h_f b + 0.85 f'_{c\,(web)}\, (a - h_f)\, b_w \quad (22)$$

If the compression and tension forces are in equilibrium, the moments can then be summed about the centroid of the prestressing steel:

$$M_n = 0.85 f'_{c\,(flange)}\, h_f b \left(d_p - \frac{h_f}{2}\right) + 0.85 f'_{c\,(web)}\, (a - h_f)\, b_w \left(d_p - h_f - \frac{a - h_f}{2}\right) \quad (23)$$

The parametric studies use Eqs. (15) to (20) for T-beams of uniform strength, and Eqs. (15) to (18) and (21) to (23) for T-beams with different concrete strengths in the flange and web.

Nonlinear Strain Compatibility Analysis

In this approach, nonlinear stress-strain relationships are used for concrete in compression. This model is shown in Fig. 4. Since the equivalent rectangular concrete compressive stress distribution is not used, β_1 is not a variable in these calculations.

As with the PCI BDM method, the depth to the neutral axis is assumed, and based on a maximum concrete compressive strain of 0.003, the strains and corresponding stresses and forces in the concrete and steel are calculated. The sum of the forces must result in equilibrium, or another value of c is chosen and the process is repeated.

The stress-strain relationship for concrete in compression is taken from Collins and Mitchell,[11] and can be written as:

$$\frac{f_c}{f'_c} = \frac{n\left(\frac{\varepsilon_{cf}}{\varepsilon'_c}\right)}{n - 1 + \left(\frac{\varepsilon_{cf}}{\varepsilon'_c}\right)^{nk}} \quad (24)$$

where:

$$n = 0.8 + \frac{f'_c}{2500} \quad (25)$$

$$k = 0.67 + \frac{f'_c}{9000} \quad (26)$$

If $\frac{\varepsilon_{cf}}{\varepsilon'_c} < 1.0$, $k = 1.0$.

$$E_c = \frac{(40{,}000\sqrt{f'_c} + 1{,}000{,}000)}{1000} \quad (27)$$

$$\varepsilon'_c(1000) = \frac{f'_c}{E_c}\left(\frac{n}{n - 1}\right) \quad (28)$$

The resulting stress-strain curves for concrete compressive strengths ranging from 5000 to 15,000 psi (34.5 to 103 MPa) are shown in Fig. 5. The depth to the neutral axis c is divided into slices, and the strain and corresponding stress are calculated at the center of each slice. The compression forces and moment arms are then computed based on the area and distance from the maximum compression fiber to the center of each slice, and the resultants are obtained for the compression forces in the flange and web.

The tension in the steel is determined by the calculated strain. For non-prestressed mild steel reinforcement, the bilinear relationship discussed in Assumption No. 4 is used. For prestressing steel, Eqs. (15) to (17) are used. The tension force must equal the compression force, or another value of c must be chosen and the process repeated. The moment capacity is then determined by summing the product of the compression forces in the flange and web and the moment arm between their resultants and centroid of the tension steel.

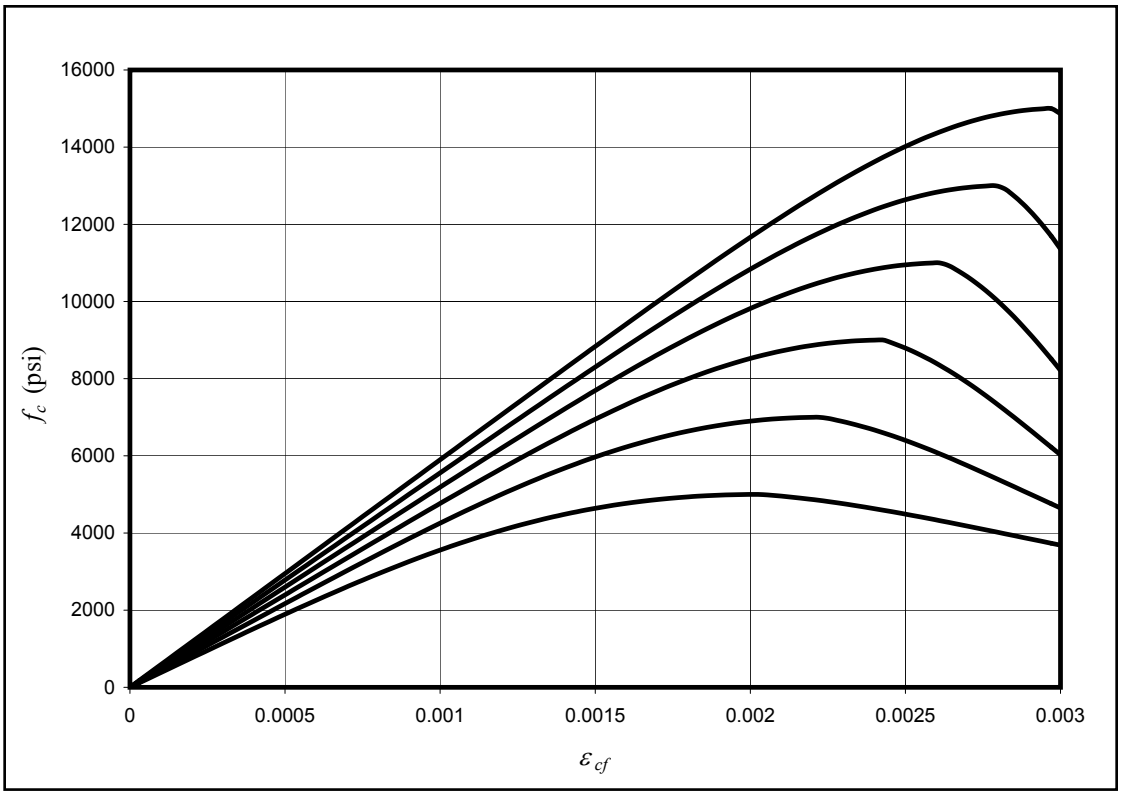

Fig. 5. Nonlinear concrete compressive stress-strain relationships per Collins and Mitchell.[11]

Approximate Methods Versus Strain Compatibility Methods

The approximate methods of LRFD and STD offer the advantage of simple closed-form solutions that can easily be incorporated into design software. The results of the approximate methods are sufficient for the majority of prestressed concrete designs, since allowable stresses usually govern. However, this simplicity can also produce overly conservative results. In many cases, actual T-beams include configurations of concrete in the compression zone and steel that cannot be accurately reflected by the simplistic models shown in Figs. 1 and 2.

Disadvantages of the approximate methods include the following:

- Typical I-girder construction includes the deck, the haunch below the deck, the girder flange and then the web. The approximate methods can model only the deck and web. The top flange of prestressed I-girders can contribute considerably to moment capacity and is often worthwhile to include in the analysis.
- The approximate methods lump reinforcement into one centroid, which cannot represent members with distributed reinforcement.
- The approximate equations cannot accommodate strands with different levels of prestressing. Today, top strands are routinely used to control camber, reduce the required concrete release strength, and enhance lateral stability of the girder. In many cases, these top strands are stressed to a different level than the bottom strands.
- The approximate equations are not valid if the effective prestress is less than $0.5f_{pu}$.
- The approximate equations cannot accommodate high strength steels other than prestressing strand.
- The approximate equations cannot accommodate different concrete strengths in the deck and girder.

Both the PCI BDM and nonlinear strain compatibility methods have the ability to address all of these disadvantages. Girgis et al.[2] give an example of a beam with high strength rods using the PCI BDM strain compatibility method. Weigel et al.[13] provide design examples of the use of the nonlinear strain compatibility method including the girder top flange.

Equivalent Rectangular Stress Block Versus Nonlinear Stress-Strain Curves

As discussed earlier, the original derivation of the equivalent rectangular concrete compressive stress distribution can be traced to Mattock et al.,[5] and subsequently to ACI 318R-83[6] and STD.[8] Mattock et al. conclude that "the proposed method of ultimate strength design permits prediction with sufficient accuracy of the ultimate strength in bending, in compression, and in combinations of the two, of all types of structural concrete sections likely to be encountered in practice." A series of derivations are provided for different types of sections, including T-beams, and comparisons are made between theory and the results of actual tests.

For T-beams, the derivation by Mattock et al. does not reduce the area of the top flange overhangs as is done in the derivation of the LRFD equations. Therefore, the method of STD is not "an interpretation of T-section behavior which, unfortunately over time, has parted from the original derivation of the rectangular stress block."[3] In fact, STD is based on the original derivation of the equivalent rectan-

gular stress block. It is the LRFD derivation that has parted from the original derivation.

Fig. 6(a) shows the concrete stress distribution in the flange, using the stress-strain relationship of Fig. 5 for 7000 psi (48.3 MPa) concrete, at a reinforcement ratio just large enough so that $c = h_f$. Up to this point, there is no difference in the calculated flexural strength of the beam using either LRFD or STD. As the reinforcement ratio increases and the neutral axis moves down the web, LRFD does not allow the compression in the flange overhangs to change from what is shown in Fig. 6(a).

The result is shown in Fig. 6(b). Clearly, strain compatibility is not being served. In reality, the high-intensity portion of the stress-strain curve covers the flange, and the stress is truncated (does not go to zero) at the bottom of the flange overhangs, as shown in Fig. 6(c).

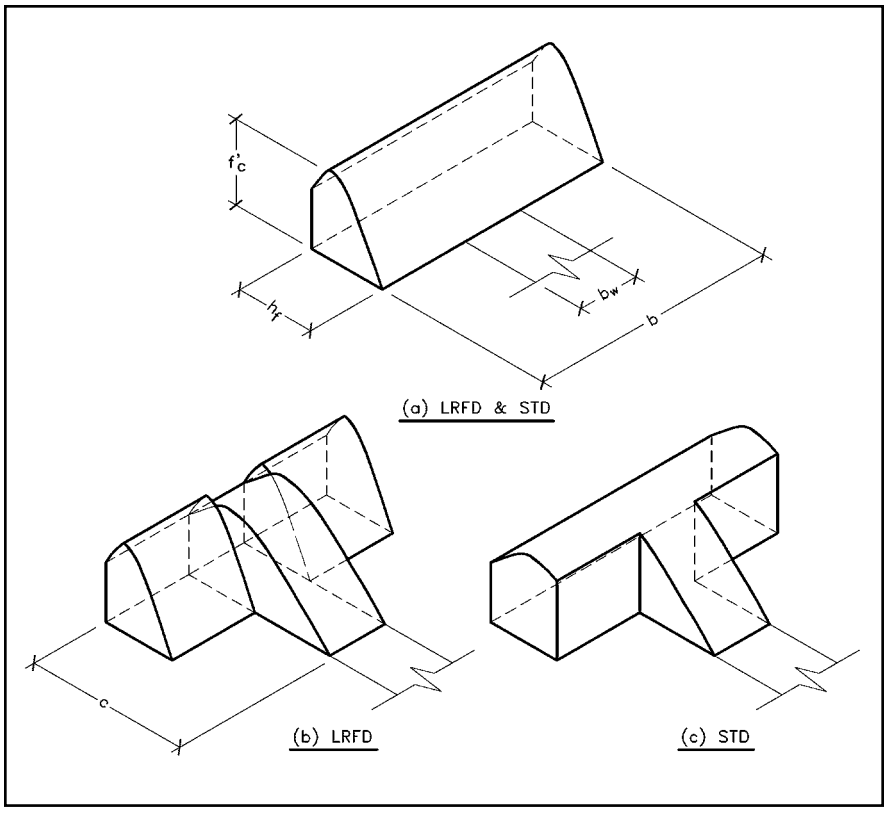

Fig. 6. Nonlinear T-beam stress distribution comparison – LRFD versus STD.

The results of the parametric study will show that the compressive stress distribution in a T-beam of uniform strength, as shown in Fig. 6(c), is accurately and conservatively predicted by a uniform stress of intensity $0.85f'_c$ over the entire area bounded by the edges of the cross section and a straight line located parallel to the neutral axis at a distance $a = \beta_1 c$ from the fiber of maximum compressive strain. This result mirrors the conclusions reached by Mattock et al. over 40 years ago.

The derivation of the equivalent rectangular concrete compressive stress distribution by Mattock et al.[5] considered the normal strength concrete (NSC) available at the time. In fact, the verification testing shown in Table 3 included T-beams with a maximum concrete strength of only 5230 psi (36.1 MPa). Extension of this work to high strength concrete (HSC) up to 15,000 psi (103 MPa) is one of the goals of this study.

Recent research by Bae and Bayrak[18] has called into question the stress block parameters of ACI 318-02,[10] and by extension STD, as they apply to HSC columns. One of the primary concerns was early spalling of the concrete cover at a compressive strain less than 0.003. Consequently, Bae and Bayrak reduced the compressive strain limit for concrete strengths greater than 8000 psi (55.2 MPa) to 0.0025, and developed new stress block parameters α_1 and β_1 for both NSC and HSC. The parameter α_1 is the stress intensity factor in the equivalent rectangular area, and is set equal to 0.85 in ACI 318-02.

The nonlinear stress-strain curves used by Bae and Bayrak were essentially the same as those used in this study. As the curves in Fig. 5 show, concrete strengths of about 10,000 psi (70 MPa) or higher will not reach their peak stress at a strain of 0.0025. At a strain of 0.003, 15,000 psi (103 MPa) concrete just barely reaches its peak stress. The resulting shapes of these stress-strain curves were not considered in the original derivation of the stress block parameters.

Bae and Bayrak conclude that the primary reason for early cover spalling is the presence of significant confinement reinforcement in the test specimens. For plain or lightly reinforced HSC specimens with concrete strengths ranging from 8700 to 18,500 psi (60 to 130 MPa), Ibrahim and MacGregor[19] reported maximum concrete strains just prior to spalling of 0.0033 to 0.0046.

Tests by Ozden[20] and Bayrak[21] of well-confined columns resulted in maximum concrete strains as low as 0.0022 prior

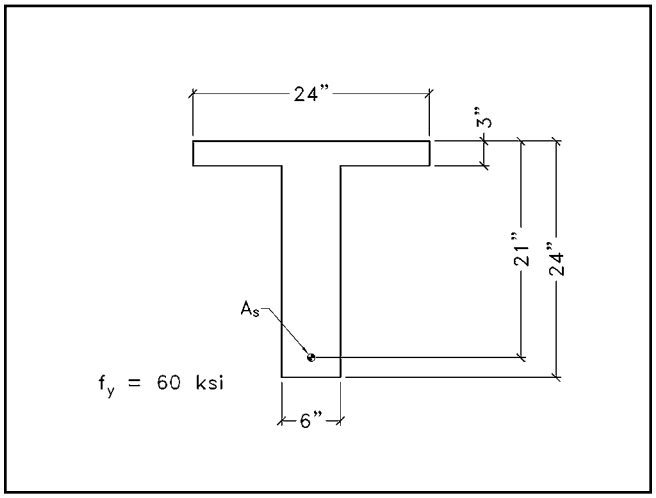

Fig. 7. Non-prestressed T-beam of uniform strength for parametric study.

to spalling. The researchers speculate that one reason for this result is that the heavy confinement causes a weak plane between the concrete core and cover. Secondly, the behavior of heavily confined and unconfined concrete is very much different, which causes high shear stresses to develop between the core and the cover.

Heavy confinement is typically not present in the compression zone of T-beams. Therefore, the authors believe the assumption of a maximum compressive strain of 0.003 is still valid for HSC T-beams. In addition, for higher strength concretes, the high-intensity portion of the curve is pushed further up into the flange, where it is more effective in resisting flexure. The parametric studies will show that, for T-beams of uniform strength up to 15,000 psi (103 MPa), the current ACI 318-02 (and STD) stress block parameters provide reasonable estimates of flexural strength.

The same cannot be said of T-beams with different concrete strengths in the flange and web. The combination of different stress-strain curves, flange thicknesses and strain gradients further distort the compression zone configuration. This will be discussed later in this paper.

Mixed AASHTO LRFD and STD Equations

The approximate analysis methods of LRFD and STD both have advantages and disadvantages. As mentioned earlier, the

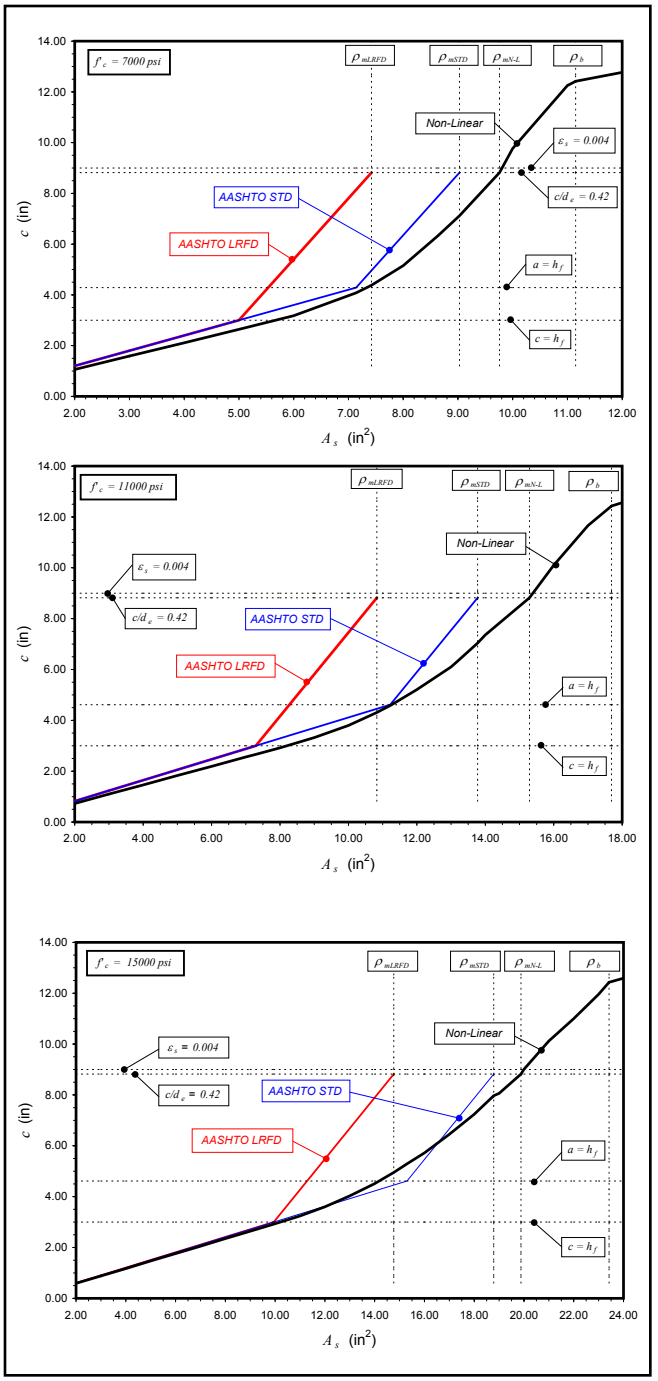

Fig. 8. Effect of steel area on depth to the neutral axis for non-prestressed T-beams of uniform strength.

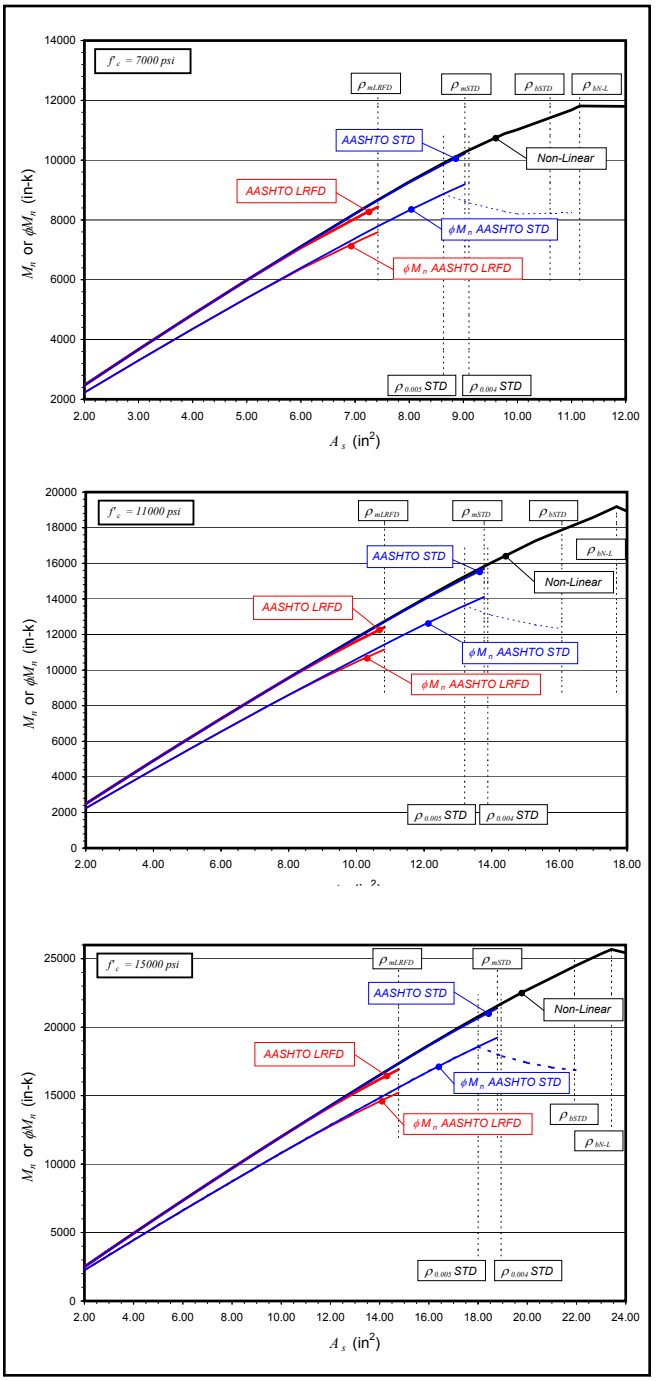

Fig. 9. Effect of steel area on nominal and design flexural strength for non-prestressed T-beams of uniform strength.

equation for the estimation of the stress in prestressing steel at nominal flexural strength, f_{ps}, given in STD can overestimate the steel stress for T-beams. The equation given in LRFD, with the depth to the neutral axis as a variable, appears to provide a reasonable and conservative estimate of this stress for T-beam behavior, if flanged behavior is assumed to begin when $a = h_f$.

On the other hand, STD provides a better model of the behavior of the flange overhangs than does LRFD. By combining the best of both methods, a more accurate approximate analysis of prestressed T-beams of uniform strength can be achieved. The proposed derivation of this "mixed" approach is as follows.

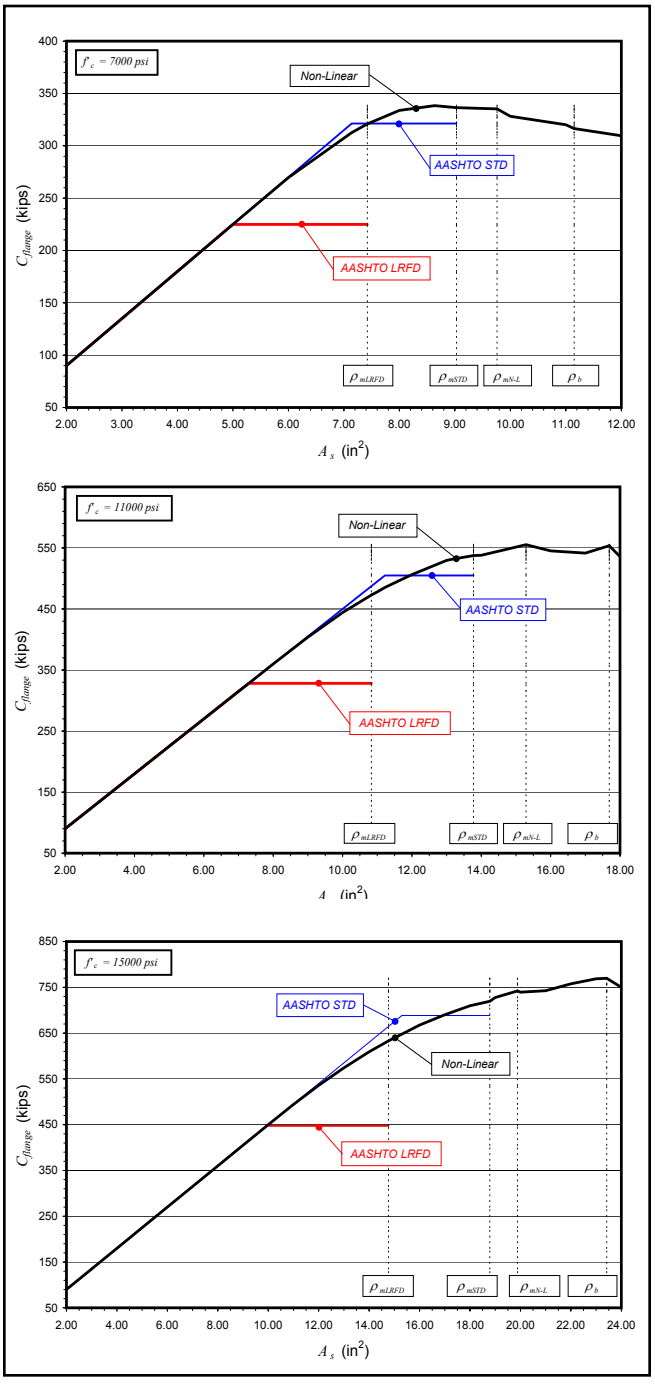

Fig. 10. Effect of steel area on compression in the flange overhangs for non-prestressed T-beams of uniform strength.

Eqs. (1) and (2) of the LRFD derivation remain unchanged. In Eq. (3), β_1 is dropped from the last term since STD does not restrict the compressive stress in the flange overhangs to the upper $\beta_1 h_f$. In following the subsequent derivation through Eqs. (4) and (5), the depth to the neutral axis can be written as:

$$c = \frac{A_{ps} f_{pu} + A_s f_y - A_s' f_y' - 0.85 f_c' (b - b_w) h_f}{0.85 f_c' b_w \beta_1 + k A_{ps} \dfrac{f_{pu}}{d_p}} \qquad (29)$$

Summing the moments about the centroid of the compression force in the web results in the same moment capacity equation as in the STD derivation [Eq. (10)]. Eqs. (1), (2), (29) and (10) are used in the parametric study of prestressed T-beams of uniform strength to assess the accuracy of the "mixed" approach. In this "mixed" approach, the only parameter that is changed from LRFD is the removal of the β_1 factor from the flange overhang term.

PARAMETRIC STUDY

Non-Prestressed T-Beams of Uniform Strength

The configuration of the T-beam investigated in this study is shown in Fig. 7, which is reproduced from Fig. C.5.7.3.2.2-1 of LRFD. This is the same section that has been discussed at length in recent issues of the PCI JOURNAL.[1] The behavior of this beam with varying mild steel tension reinforcement ratios is compared using three methods: LRFD, STD, and the nonlinear strain compatibility analysis.

To determine the influence of concrete strength on the results, strengths of 7000 to 15,000 psi (48.3 to 103 MPa) are considered in 4000 psi (27.6 MPa) increments. The results are plotted in Figs. 8 to 10. Each figure contains three charts for comparison purposes, each chart representing a concrete strength within the noted range.

The vertical lines labeled ρ_m represent the maximum reinforcement ratios for LRFD, STD, and the nonlinear analysis based on a maximum c/d_e ratio of 0.42, which is the limit prescribed by LRFD. Although the curves representing LRFD and STD are discontinued at their respective maximum reinforcement limits, the curves representing the nonlinear analysis are continued to the right of the line labeled $\rho_{mN\text{-}L}$ to observe the behavior beyond the maximum reinforcement limit. In design, mild steel tension reinforcement quantities beyond the respective maximum reinforcement limits are currently not allowed.

The vertical lines labeled ρ_b represent balanced conditions, where the stress in the tension steel reaches yield at the same time the strain in the maximum compression fiber reaches 0.003. The sudden change in behavior of the nonlinear curves beyond the lines labeled ρ_b or $\rho_{bN\text{-}L}$ reflects that the mild steel tension reinforcement has not reached its yield strain.

Depth to the Neutral Axis—Fig. 8 plots the depth to the neutral axis against the area of mild steel tension reinforcement. The nonlinear analysis indicates a smooth transition between rectangular and T-beam behavior, contrary to the sudden change in slope predicted by both LRFD and STD. However, in general, the depth to the neutral axis calculated with the nonlinear analysis is smaller than that determined

Table 1. Moment capacity comparison for AASHTO STD and the nonlinear analysis.

f'_c (ksi)	A_s (sq in.)	AASHTO STD						Nonlinear						$\frac{M_{nSTD}}{M_{nN\text{-}L}}$
		c (in.)	C_{flange} (kips)	C_{web} (kips)	y_{flange} (in.)	y_{web} (in.)	M_{nSTD} (kip-in.)	c (in.)	C_{flange} (kips)	C_{web} (kips)	y_{flange} (in.)	y_{web} (in.)	$M_{nN\text{-}L}$ (kip-in.)	
15	13.00	3.92	585.0	195.0	1.27	1.27	15386	4.03	574.2	205.8	1.23	1.38	15390	1.000
15	14.00	4.22	630.0	210.0	1.37	1.37	16487	4.51	609.2	230.8	1.28	1.54	16504	0.999
15	14.77	4.46	664.6	221.5	1.45	1.45	17325	4.95	633.0	253.1	1.31	1.69	17351	0.999
15	15.30	4.62	688.5	229.5	1.50	1.50	17901	5.29	647.8	270.3	1.32	1.81	17932	0.998
15	16.00	5.46	688.5	271.5	1.50	1.77	18645	5.72	667.5	292.5	1.35	1.96	18686	0.998

Note: 1 ksi = 6.895 MPa; 1 sq in. = 645 mm^2; 1 in. = 25.4 mm; 1 kip = 4.448 kN; 1 kip-in. = 0.113 kN-m.

Table 2. Non-prestressed maximum moment capacity comparison.

	f'_c (ksi)		
	7.0	11.0	15.0
	Nominal moment strength (kip-in.)		
M_{nLRFD}	8435	12,404	16,915
M_{nSTD}	10,214	15,678	21,379
$M_{nN\text{-}L}$	10,885	17,261	22,628
$\frac{M_{nLRFD}}{M_{nN\text{-}L}}$	0.77	0.72	0.75
$\frac{M_{nSTD}}{M_{nN\text{-}L}}$	0.94	0.91	0.94

Note: 1 ksi = 6.89 MPa; 1 kip-in. = 0.113 kN-m.

by either LRFD or STD, with STD providing the closer approximation.

An exception to this behavior is shown in Fig. 8 for 15,000 psi (103 MPa) concrete. The nonlinear curve crosses the STD curve at a smaller steel area than where STD assumes flanged section behavior to begin. For comparison purposes, Table 1 shows the relevant data for both calculation methods in this range of steel areas. Although the nonlinear analysis predicts slightly larger depths to the neutral axis at some steel quantities, the ratio of the STD calculated moment capacities to the nonlinear calculated capacities ranges from 0.998 to 1.000. Thus, the STD prediction method is accurate in this range of concrete strengths and steel areas.

Nominal Flexural Strength—Fig. 9 plots calculated moment capacity, M_n, against the area of mild steel tension reinforcement. In no case does the moment capacity calculated according to STD exceed that computed by the nonlinear analysis. Up to the limit of ρ_{mSTD}, the ratio of the STD calculated moment capacities to the nonlinear calculated capacities ranges from 0.975 to 1.000. For LRFD, this range is 0.961 to 1.000.

At first glance, the differences between the three calculation methods do not appear to be significant. However, when viewed from the perspective of maximum reinforcement ratios, the differences become larger. Table 2 compares the maximum allowable moment capacity for each of the three methods, based on a maximum c/d_e ratio of 0.42, for each concrete strength. The STD method represents a 6 to 9 percent reduction in maximum moment capacity of the section when compared to the nonlinear analysis. LRFD represents a 23 to 28 percent reduction.

The design flexural strengths, ϕM_n, calculated according to LRFD and STD are also shown in Fig. 9. Resistance factors and maximum reinforcement limits will be discussed later in this paper.

Compression in the Top Flange Overhangs—As mentioned earlier in this paper, LRFD contends that once the depth to the neutral axis exceeds the flange depth, the flange overhangs can accept no additional compressive force from the moment couple. Fig. 10 plots the force in the flange overhangs against the area of mild steel tension reinforcement. According to the nonlinear analysis, the flange overhangs can accept significantly more compression than LRFD predicts. As the neutral axis moves down the web, the high-intensity portion of the compressive stress-strain curve covers the flange, generally resulting in an average stress of $0.85f'_c$ or higher.

It can also be seen in Fig. 10 that STD provides a conservative prediction of the force in the flange overhangs, except at roughly the reinforcement ratio where STD predicts T-beam behavior to begin. Here, the nonlinear curve cuts below the STD curve. This behavior becomes more severe as the concrete strength increases. However, as shown in Fig. 5, as the concrete strength increases, the high-intensity portion of concrete stress-strain curve also moves closer to the fiber of maximum compressive strain.

Although the nonlinear analysis predicts a lower force in the flange overhangs in this range, the moment arm of the resultant force is larger than predicted by STD. This effect can be seen in Table 1, where y_{flange} is the distance from the extreme compression fiber to the centroid of the compression force in the flange overhangs. The net result is that the moment capacities calculated with STD are accurate on the conservative side when compared to the nonlinear analysis.

Prestressed T-Beams of Uniform Strength

The configuration of the T-beams investigated in this study is shown in Fig. 11, which is similar to the section discussed

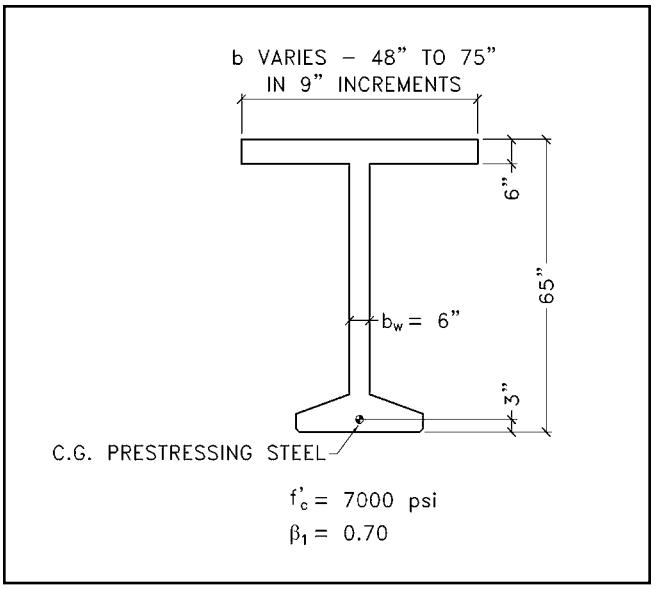

Fig. 11. Prestressed T-beam of uniform strength for parametric study.

in Reference 1, except that the width of the top flange is varied from 48 to 75 in. (1220 to 1905 mm) in 9 in. (229 mm) increments to investigate the effect of the compression flange width on T-beam behavior. The behavior of these beams with varying prestressing steel quantities is compared using five methods: LRFD, STD, mixed LRFD/STD, PCI BDM, and the nonlinear strain compatibility analysis.

The results of this study are plotted in Figs. 12 to 15. Each figure consists of two charts showing the narrowest and widest flange widths considered at a constant design concrete strength of 7000 psi (48.3 MPa). In the interest of saving space, plots for the intermediate flange widths are not shown. However, the same trends are exhibited with the intermediate flange widths as with the extreme flange widths. In general, because of the $\beta_1 h_f$ restriction on the compressive area depths in the flange overhangs, the penalty associated with the LRFD method becomes more severe with wider flanges.

Depth to the Neutral Axis—Fig. 12 plots the depth to the neutral axis against the area of prestressing steel. In general, for any given reinforcement ratio, the depth to the neutral axis calculated with the nonlinear analysis is smaller than that determined by any of the other prediction methods. Assuming the nonlinear analysis to be the most exact, the mixed LRFD/STD and PCI BDM methods provide reasonably good estimates of the depth to the neutral axis. The LRFD method provides the poorest prediction.

Steel Stress at Nominal Flexural Strength—Since the stress in the prestressing steel is nonlinear, it must be predicted by any of the calculation methods. Fig. 13 plots the predicted stress in the prestressing steel at nominal flexural strength against the area of steel for the five methods. Assuming the nonlinear analysis provides the best prediction, the PCI BDM method provides the next-best prediction. Again, LRFD provides the poorest prediction.

The LRFD equations would provide a reasonable estimate of the stress in the prestressing steel at nominal strength if T-beam behavior were assumed to begin when $a = h_f$. This

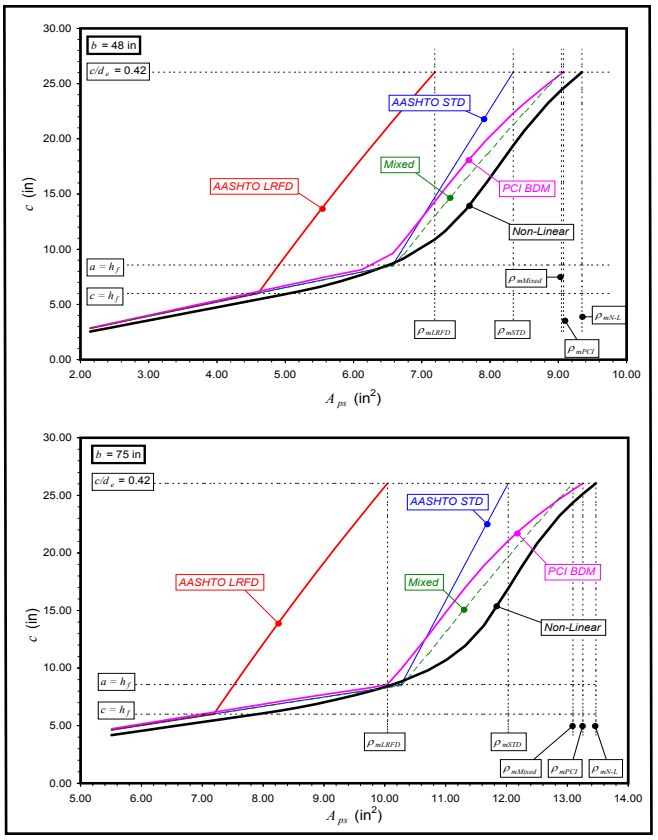

Fig. 12. Effect of steel area on depth to the neutral axis for prestressed T-beams of uniform strength.

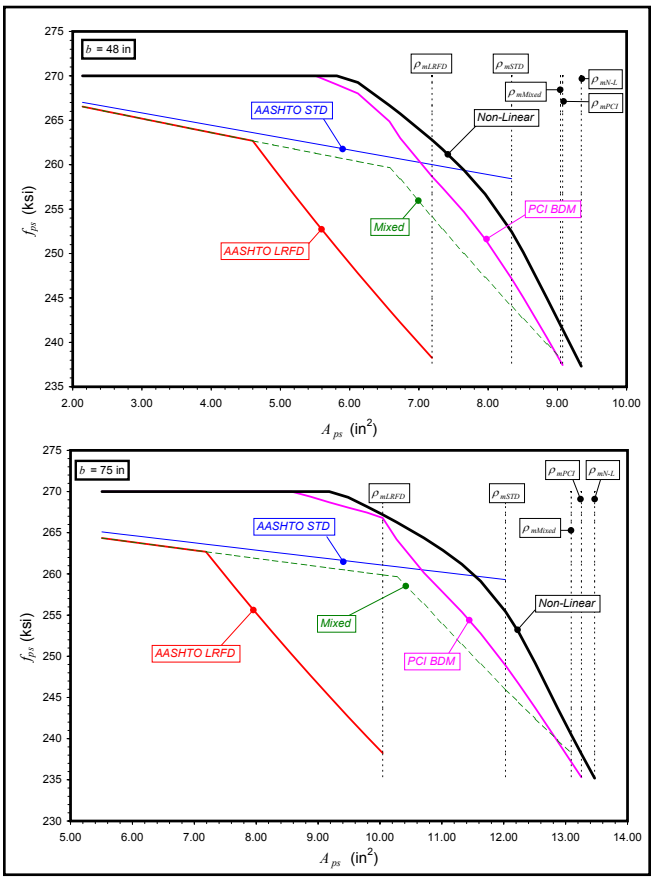

Fig. 13. Effect of steel area on stress in the prestressing steel at nominal flexural strength for prestressed T-beams of uniform strength.

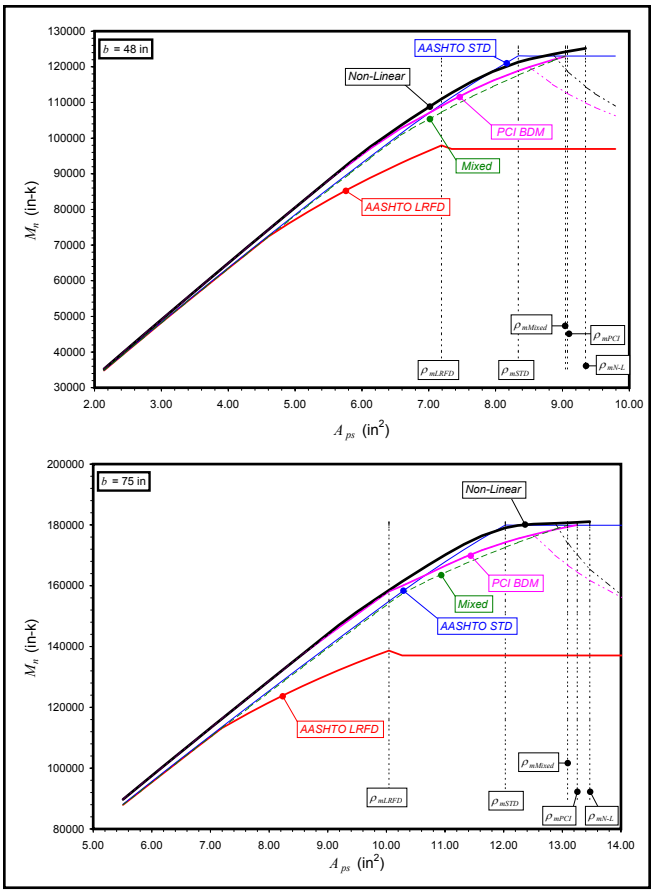

Fig. 14. Effect of steel area on nominal flexural strength for prestressed T-beams of uniform strength.

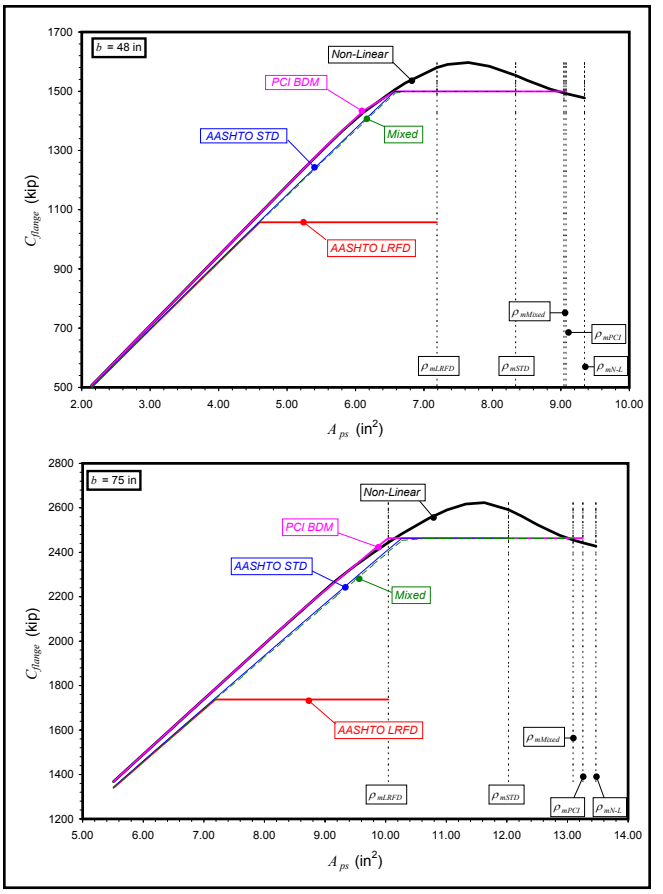

Fig. 15. Effect of steel area on compression in the flange overhangs for prestressed T-beams of uniform strength.

is part of the mixed LRFD/STD proposal, and is shown by the dashed line in the charts. Also note that since the STD equation does not vary with the depth to the neutral axis, it provides a linear estimate of the steel stress that overstates the value of f_{ps} at higher reinforcement ratios.

Nominal Flexural Strength—Fig. 14 plots the calculated moment capacity against the area of prestressing steel. Due to the overestimation of f_{ps}, the STD method tends to overestimate the moment capacity as the reinforcement ratio approaches ρ_{mSTD}. Compared to the nonlinear analysis, both the mixed LRFD/STD and PCI BDM methods provide reasonable estimates, both of moment strength and the maximum reinforcement ratio. The LRFD method predicts significantly lower moment strengths and maximum reinforcement ratios.

Beyond their respective maximum reinforcement ratios, the curves for both LRFD and STD level off, indicating that over-reinforced prestressed sections are allowed, but with their design strength limited to the maximum for an under-reinforced section. The dash-double dot lines originating from the nonlinear and PCI BDM curves consider a variable resistance factor to reflect member ductility, which will be discussed later in this paper.

Compression in the Top Flange Overhangs—Finally, Fig. 15 plots the compressive force in the top flange overhangs against the area of prestressing steel. With the exception of LRFD, all of the methods show good agreement with the nonlinear analysis.

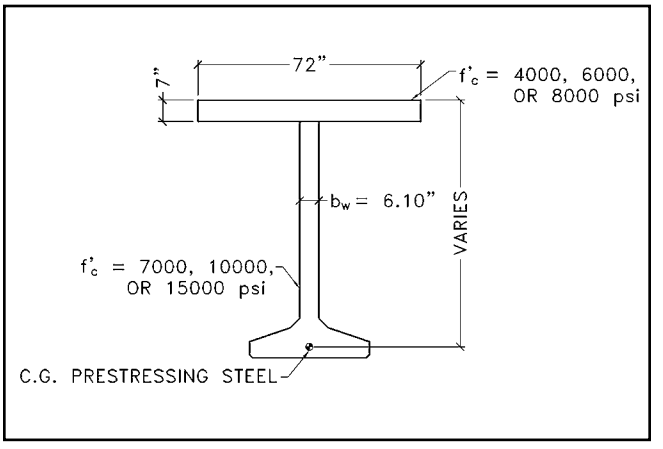

Fig. 16. Prestressed T-beam with different concrete strengths in the flange and web for parametric study.

Composite Prestressed T-Beams

Neither LRFD nor STD provides design equations for the flexural strength of composite T-beams where the strength of the concrete in the flange is different than that in the web. The proposed revisions to the specifications shown in Appendix C can be conservatively applied assuming f'_c is the weaker of the deck and web concrete strengths. If a more refined analysis is desired, the PCI BDM offers a strain compatibility method that uses an area-weighted average β_1 to determine the depth of the equivalent rectangular stress distribution.

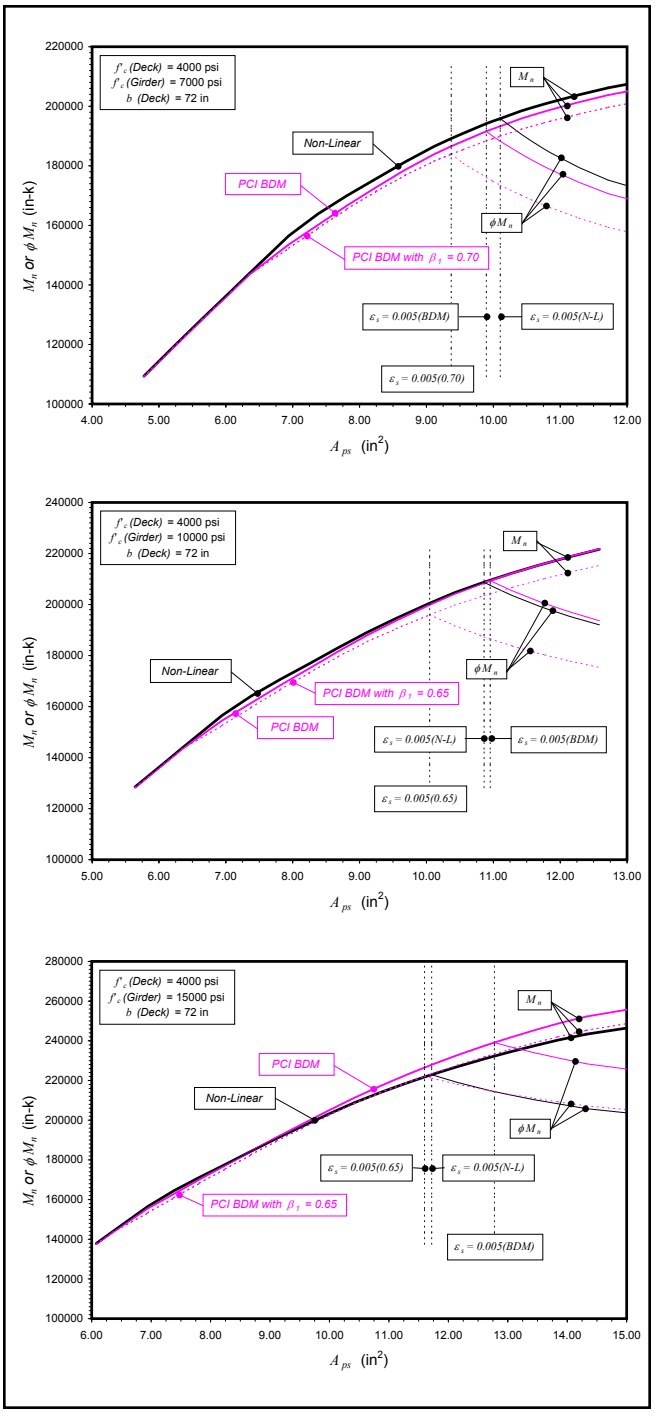

Fig. 17. Effect of steel area on nominal and design flexural strength for variable strength prestressed beams with a 4000 psi (27.6 MPa) deck.

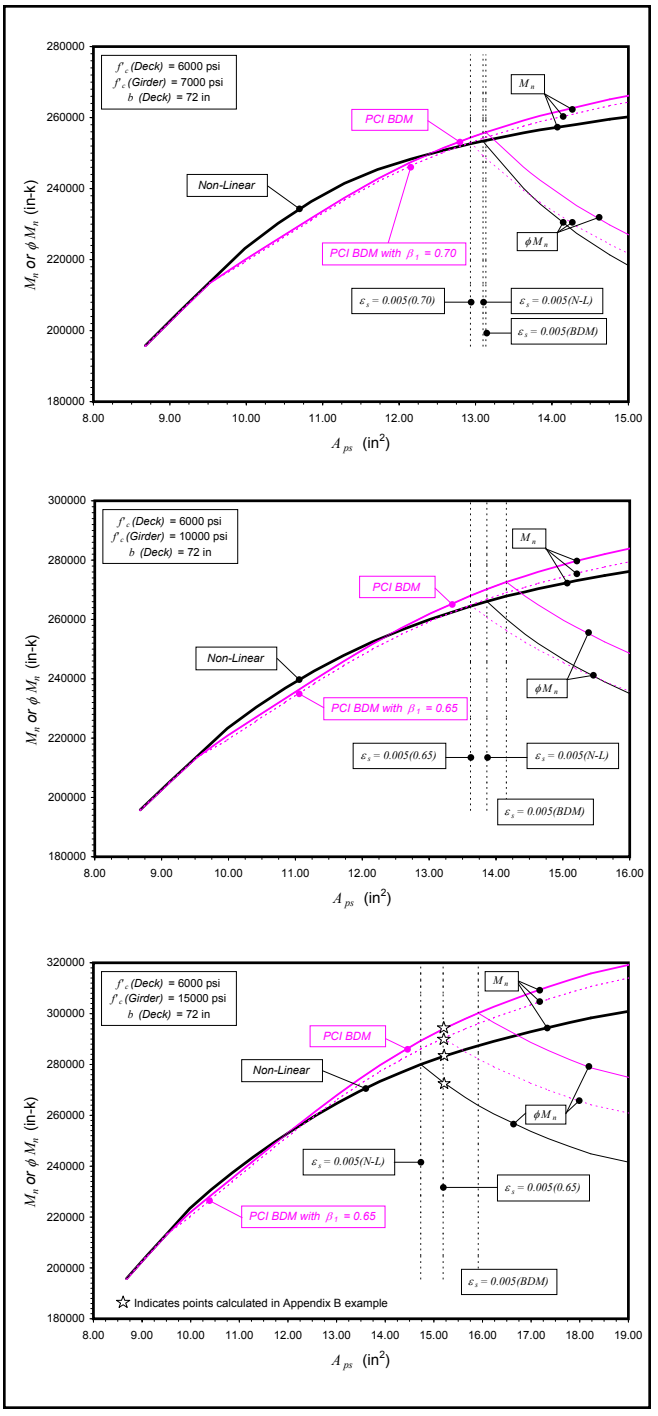

Fig. 18. Effect of steel area on nominal and design flexural strength for variable strength prestressed beams with a 6000 psi (41.4 MPa) deck.

The accuracy of the average β_1 approach has not been verified in the literature. Consequently, a parametric study was performed on the section shown in Fig. 16, which is a WSDOT W83G girder (ignoring the top flange) at a 6 ft (1.83 m) spacing made composite with a 7 in. (178 mm) thick structural deck. The eccentricity of the prestressing steel is allowed to vary in accordance with the standard strand pattern established for these members.

The results of the PCI BDM and nonlinear strain compatibility analyses are plotted in Figs. 17 to 19 for deck strengths of 4000, 6000 and 8000 psi (27.6, 41.4 and 55.2 MPa) and girder strengths of 7000, 10,000 and 15,000 psi (48.3, 69.0 and 103 MPa). In addition, where the value of β_1 of the girder concrete is different than that of the deck concrete, a curve is also plotted representing the PCI BDM method using β_1 of the girder concrete instead of the average β_1 value.

For a 4000 psi (27.6 MPa) deck, Fig. 17 shows that the PCI BDM gives reasonable estimates of flexural strength for girder strengths up to 10,000 psi (69.0 MPa). At a girder strength of 15,000 psi (103 MPa), the PCI BDM method overestimates the flexural strength at higher reinforcement ratios when compared to the nonlinear analysis. In all cases where

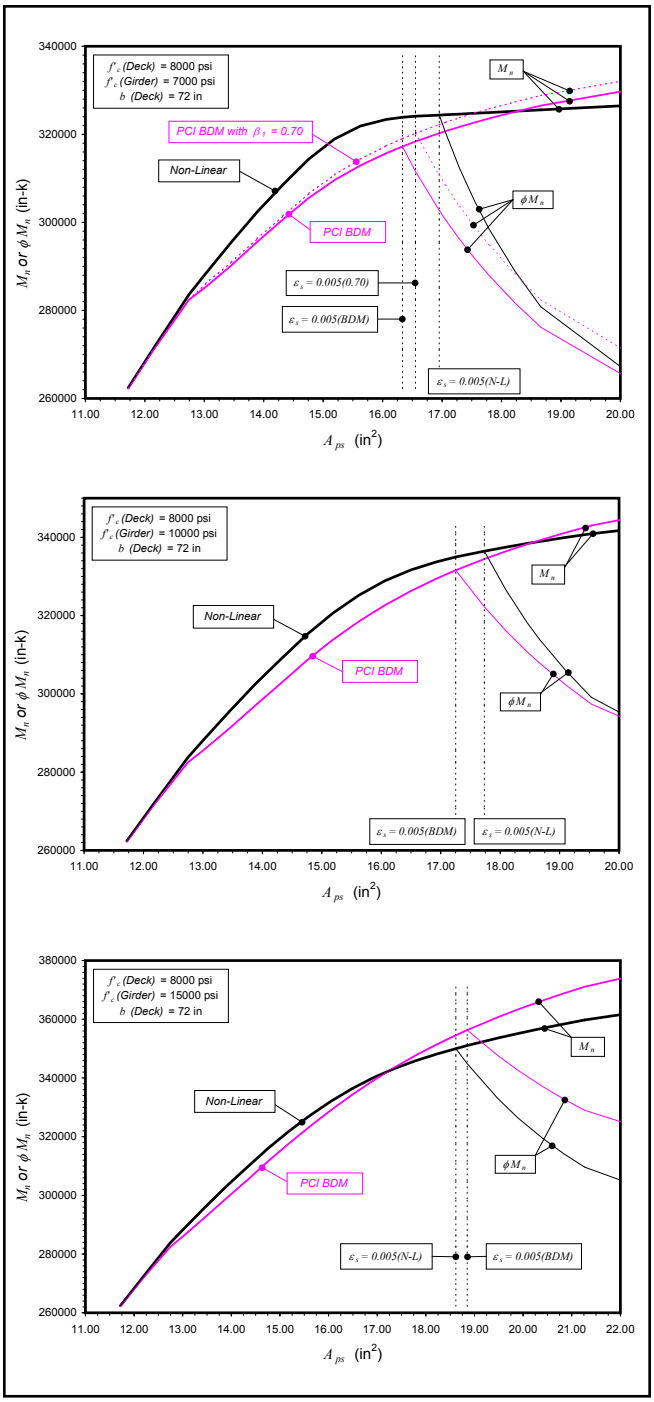

Fig. 19. Effect of steel area on nominal and design flexural strength for variable strength prestressed beams with an 8000 psi (55.2 MPa) deck.

the girder concrete is stronger than the deck, and where β_1 for the girder is different than for the deck, using β_1 for the girder concrete in the calculations provides a more conservative estimate than the average β_1 approach. For the 15,000 psi (103 MPa) girder with a 4000 psi (27.6 MPa) deck, using β_1 for the girder concrete provides a reasonable estimate of the strength of the composite section.

Fig. 18 shows that, for a 6000 psi (41.4 MPa) deck, the PCI BDM method provides a reasonable estimate for the flexural strength of the composite section at low reinforcement ratios, but overestimates the strength at higher reinforcement ratios.

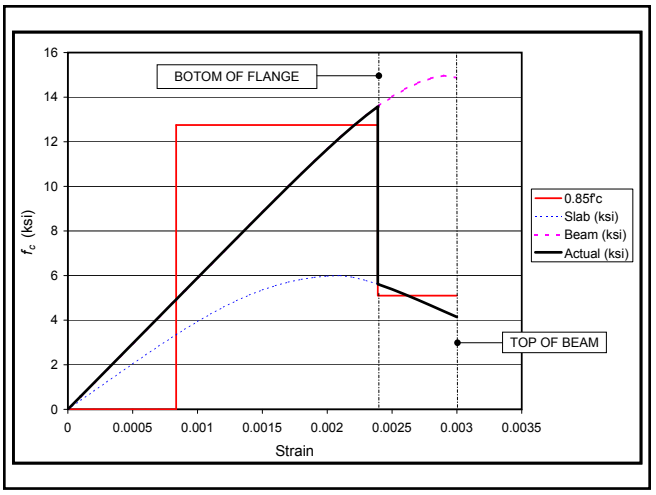

Fig. 20. Comparison of compression zones for a prestressed T-beam with a 6000 psi (41.4 MPa) deck and 15,000 psi (103 MPa) web – PCI BDM versus nonlinear analysis.

This trend becomes more pronounced as the girder strength increases. The same can be said of the PCI BDM curves using β_1 of the girder concrete.

The reason for the overestimation of strength is shown in the example of Appendix B, which calculates the flexural strength of a 15,000 psi (103 MPa) girder with a 6000 psi (41.4 MPa) deck. These calculations correspond to the vertical line in Fig. 18 labeled ε_s = 0.005(0.65) for 15,000 psi girder concrete. The PCI BDM method overestimates the compression in the deck, as well as the height of the compression resultant in the web, when compared to the nonlinear analysis.

As shown in Fig. 20, the strain gradient for this particular case cuts off the peak of the nonlinear stress-strain curves in both the deck and web. The result is an average stress of about $0.82f_c'$ in the deck, versus $0.85f_c'$ in the PCI BDM analysis. The shape of the curve in the web resembles a triangle much more closely than the truncated curve of Fig. 6, resulting in a drop in the resultant location. Both of these factors contribute to the lower calculated strength of the nonlinear analysis.

The curves for the 8000 psi (55.2 MPa) deck in Fig. 19 show the same general trends as noted above. Therefore, for different concrete strengths in the flange and web, the equivalent rectangular stress distribution does not yield a reliable estimate of the flexural strength of a composite section, and can in fact become unconservative. The different shapes of the stress-strain curves combined with a variable flange thickness and strain gradient can result in nonlinear compression block configurations that are not accurately modeled with the traditional β_1 approach.

The parametric studies were done using spreadsheets for both the PCI BDM and nonlinear analyses. Although the nonlinear spreadsheet was somewhat more difficult to develop than the PCI BDM spreadsheet, it is not any more difficult to use. The authors recommend that, where an accurate estimate of the flexural strength of composite T-beams is required, a nonlinear analysis similar to the one used in this study be employed. The Washington State Department of Transporta-

tion (WSDOT) publishes a subroutine library of the analysis methods presented in this paper at www.wsdot.wa.gov/eesc/bridge. The subroutine library, called WBFL, can be used in spreadsheets and other programming systems.

MAXIMUM REINFORCEMENT LIMITS AND ϕ FACTORS

Current maximum reinforcement limits for flexural members are intended to ensure that the tension steel yields at nominal flexural strength. This yielding is generally considered to result in ductile behavior, with large deflections, cracking and ample warning of impending failure. However, as currently applied, the inconsistency inherent with these limits is that under-reinforced sections are required for non-prestressed beams, but not for columns or prestressed beams.

To remedy this inconsistency, Mast[15] proposed revisions to ACI 318-89[16] that would unify the design of reinforced and prestressed concrete flexural and compression members. A modified version of this proposal was adopted as Appendix B in ACI 318-95,[17] and was moved to the body of the code in ACI 318-02.[10]

Concrete sections are now defined in ACI 318 as "tension-controlled" (beams) when, at nominal strength, the net tensile strain in the extreme tension steel is at least 0.005. Members are "compression-controlled" (columns) when the net tensile strain in the extreme tension steel at nominal strength is less than or equal to 0.002 (for Grade 60 and all prestressed reinforcement).

In between, there is a transition zone where the resistance factor can be reduced linearly between ϕ for tension-controlled sections and ϕ for compression-controlled sections. This reduction in ϕ reflects, in part, the reduced ductility of the member as the reinforcement ratio increases. It is not uncommon for codes and specifications to allow overstrength to compensate for a reduction in ductility.

Extreme Depth Versus Effective Depth—The net tensile strain in the steel at nominal strength is determined in ACI 318-02 at the extreme depth, d_t, which is the distance from the extreme compression fiber to the steel closest to the tension face. In LRFD, the current maximum reinforcement limit is based on $c/d_e \le 0.42$, where d_e is defined as the distance from the extreme compression fiber to the centroid of the tension force. This difference has been discussed at length in the literature, most recently in Reference 25, which proposes changing the extreme depth to effective depth in ACI 318, among other items.

The application of extreme depth appears to be misunderstood in this proposal. First, it is not used in flexural strength calculations, so it has no role in "properly accounting for the resulting tensile force in the reinforcement that is so essential for equilibrium conditions."[25] Instead, d_t is used only in the determination of ϕ, which is intended to adjust member resistance for such factors as member ductility. Also, for a column with reinforcement distributed around the perimeter, the balanced condition is generally considered to be the point at which the extreme steel yields. To provide a smooth transition between beam and column design, a consistent definition of balanced strain conditions is necessary.

The behavior of a beam at failure is not ductile, as the failure is generally sudden whether the steel ruptures or the concrete crushes. It is the behavior of the beam leading up to failure that is important. Mast[15] states that "it is desired that a flexural member have good behavior (limited cracking and deflection) at service load. It is also desired that a flexural member have the opposite type of behavior (gross cracking, large deflection) prior to reaching nominal strength, to give warning of impending failure." He believes that "the strain at extreme depth is a better indication of ductility, cracking potential and crack width" than the strain at effective depth.

The authors agree with this premise. The type of behavior that a maximum reinforcement limit is intended to preclude is where a large quantity of reinforcement near the tension face disguises the signs of impending failure until the concrete at the compression fiber crushes. Mast also points out that, for a given depth of beam, a net tensile strain not less than 0.005 at extreme depth "would give the same minimum amount of curvature at nominal strength for all tension-controlled flexural members." This type of consistent behavior is especially desirable when applying resistance factors.

Reference 25, Appendix B, gives a series of examples of rectangular beams with the primary flexural reinforcement lumped at mid-depth, and with little or no reinforcement at extreme depth. These examples are purported to show "flaws or errors" in the ACI 318-02 approach. Beams with no reinforcement at extreme depth are shown to be in the transition region according to ACI 318-02, while beams with added reinforcement at extreme depth jump back into the tension-controlled region. This result is inconsistent with previous maximum reinforcement limits.

The authors disagree with this interpretation. ACI 318-02 was not intended to be consistent with previous maximum reinforcement limits. Both types of beams will exhibit gross cracking and large deflections leading up to failure. In fact, the beam with no reinforcement at extreme depth could conceivably give the most warning of impending failure.

Accordingly, it could be argued that the beginning of the transition region should be based on the theoretical strain at the extreme tension face, rather than at extreme depth. Although the authors are not proposing this change, we believe that the net tensile strain at extreme depth is more representative of beam ductility leading up to failure than the net tensile strain at effective depth.

Non-Prestressed Beams—A maximum reinforcement ratio of $0.75\rho_b$ has been traditionally considered adequate to provide ductile behavior, and is the limit specified in STD and editions of the ACI Code through ACI 318-99.[14]

For rectangular sections with Grade 60 reinforcement, the traditional limit of $0.75\rho_b$ equates to a net tensile strain at the centroid of the steel of 0.00376. This strain is significantly higher for T-beams. ACI 318-02 requires a minimum net tensile strain in the extreme tension steel of 0.004. This is slightly more conservative than the traditional limit. The LRFD specified limit of $c/d_e \le 0.42$ equates to a minimum net tensile strain at the centroid of the tension reinforcement of 0.00414.

Mast's original proposal did not include an upper limit on the reinforcement ratio in non-prestressed beams. The intent

was to provide a smooth transition between the design of tension-controlled and compression-controlled members. Fig. 9 shows the design flexural strength (ϕM_n) of non-prestressed T-beams calculated by LRFD and STD with $\phi = 0.90$. The dashed line emanating from the intersection of the lines labeled "ϕM_n *AASHTO STD*" and "$\rho_{0.005}$ *STD*" is the design flexural strength when ϕ varies linearly from 0.90 at a net tensile strain of 0.005 to 0.70 at a net tensile strain of 0.002, 0.70 being the resistance factor specified for tied compression members in AASHTO STD.

Fig. 9 shows that, below a net tensile strain of 0.005, the design flexural strength of the T-beam decreases with increasing tension reinforcement. In this case, decreasing ductility is offset with increasing over-strength. It would not be economical for designers to continue adding tension reinforcement to the detriment of design strength. For all intents and purposes, a minimum net tensile strain of 0.005 provides a practical limit on the reinforcement ratio of non-prestressed T-beams. For a given section, only the addition of compression reinforcement would result in an increase in the nominal flexural strength.

Prestressed Beams—Fig. 14 plots the nominal flexural strength (M_n) of T-beams of uniform strength using the five different methods discussed earlier. Since for precast, pretensioned members, both LRFD and STD specify $\phi = 1.0$ for flexure, these curves also represent the design strength of the members (ϕM_n). At the respective reinforcement ratios where $c/d_e = 0.42$, both the LRFD and STD curves flatten out at the maximum moment capacity of an under-reinforced section. No guidance is given in either specification for the value of ϕ above this limit, so $\phi = 1.0$ is used for illustration purposes.

The PCI BDM and nonlinear curves terminate at the reinforcement ratio where $c/d_e = 0.42$. However, the dashed-double dot lines in the upper right hand corner represent the design flexural strengths with a varying ϕ as described for non-prestressed beams. Again, the design flexural strength decreases as the net tensile strain in the steel drops below 0.005. The results would look about the same for the LRFD/STD mixed method.

All Beams—The authors recommend the elimination of maximum reinforcement limits and the adoption of a linearly varying ϕ in the AASHTO LRFD Specifications. This is a more rational approach that provides guidance for the value of the resistance factor in the transition zone between tension-controlled and compression-controlled members.

Currently, ϕ for both tied and spirally reinforced compression members is 0.75 in LRFD. Consequently, the authors recommend $\phi = 0.75$ at a net tensile strain of 0.002. Appendix C contains proposed specification revisions to implement this change.

For non-prestressed members, ϕ in the transition region can be determined by:

$$\phi = 0.65 + 0.15\left(\frac{d_t}{c} - 1\right) \tag{30}$$

but not greater than 0.90 or less than 0.75. For prestressed members, ϕ in the transition region can be determined by:

$$\phi = 0.583 + 0.25\left(\frac{d_t}{c} - 1\right) \tag{31}$$

but not greater than 1.0 or less than 0.75.

For partially prestressed members, the conservative approach would be to use ϕ for non-prestressed members.

Table 3. T-beam test parameters from Mattock et al.[5]

Source	Beam	b (in.)	d (in.)	b_w (in.)	h_f (in.)	A_s (sq in.)	f'_c (ksi)	f_y (ksi)	M_{test} (kip-in.)
A. N. Talbot	1	16.00	10.00	8.00	3.25	1.68	1.89	54.9	922
	2	32.00	10.00	8.00	3.25	3.36	1.87	53.8	1610
	3	24.00	10.00	8.00	3.25	2.24	1.76	52.7	1107
	4	16.00	10.00	8.00	3.25	1.76	1.33	38.3	630
	5	32.00	10.00	8.00	3.25	3.36	1.19	53.4	1656
	6	24.00	10.00	8.00	3.25	2.20	1.61	38.3	773
	7	16.00	10.00	8.00	3.25	1.76	1.45	38.3	578
	8	24.00	10.00	8.00	3.25	2.20	1.75	40.7	785
	9	32.00	10.00	8.00	3.25	3.08	1.61	38.3	1005
S. A. Guralnick	IA-IR	23.00	11.81	7.00	4.00	2.08	3.23	87.7	2072
	IB-IR	23.00	11.81	7.00	4.00	1.20	2.44	84.6	1440
	IC-IR	23.00	11.78	7.00	4.00	3.72	4.93	83.9	3226
	ID-IR	23.00	11.81	7.00	4.00	2.08	4.93	87.7	2182
J. R. Gaston and E. Hognestad	1	9.00	16.25	3.50	2.75	1.20	4.73	90.0	1675
	2	9.00	16.00	3.50	2.75	1.60	5.23	90.0	2229

Note: 1 ksi = 6.895 MPa; 1 sq in. = 645 mm^2; 1 in. = 25.4 mm; 1 kip-in. = 0.113 kN-m.

Table 4. Comparison with test results from Mattock et al.[5]

Source	Beam	β_1	AASHTO LRFD			AASHTO STD			Nonlinear		
			c (in.)	M_n (kip-in.)	$\frac{M_{test}}{M_n}$	c (in.)	M_n (kip-in.)	$\frac{M_{test}}{M_n}$	c (in.)	M_n (kip-in.)	$\frac{M_{test}}{M_n}$
A. N. Talbot	1*	0.85	5.19	748	1.23	4.62	755	1.22	3.70	780	1.18
	2*	0.85	6.97	1439	1.12	5.25	1479	1.09	3.70	1533	1.05
	3*	0.85	5.10	977	1.13	3.96	986	1.12	3.31	1014	1.09
	4*	0.85	5.52	540	1.17	4.95	546	1.15	3.81	567	1.11
	5*	0.85	16.34	922	1.80	14.62	1042	1.59	6.66	1162	1.43
	6	0.85	3.02	735	1.05	3.02	735	1.05	2.56	750	1.03
	7*	0.85	4.79	555	1.04	4.22	559	1.03	3.41	576	1.00
	8	0.85	2.95	783	1.00	2.95	783	1.00	2.52	799	0.98
	9	0.85	3.17	1021	0.98	3.17	1021	0.98	2.69	1044	0.96
S. A. Guralnick	IA-IR	0.85	3.40	1891	1.10	3.40	1891	1.10	3.14	1914	1.08
	IB-IR	0.85	2.50	1091	1.32	2.50	1091	1.32	2.21	1104	1.30
	IC-IR*	0.80	4.10	3171	1.02	4.03	3171	1.02	3.81	3188	1.01
	ID-IR	0.80	2.36	1982	1.10	2.36	1982	1.10	2.22	1987	1.10
J. R. Gaston and E. Hognestad	1*	0.81	5.11	1578	1.06	4.12	1592	1.05	3.75	1601	1.05
	2*	0.79	7.42	1981	1.13	6.26	2022	1.10	5.55	2038	1.09

Note: 1 in. = 25.4 mm; 1 kip-in. = 0.113 kN-m.

* Denotes T-beams where $c > h_f$ at nominal flexural strength.

However, LRFD Eqs. 5.5.4.2.1-1 and 5.5.4.2.1-2 allow for the calculation of ϕ for flexure based on the proportion of prestressing to total steel. This value, which is between 0.90 and 1.0, can alternatively be used at a net tensile strain of 0.005. This resistance factor would then be varied linearly to 0.75 at a net strain of 0.002.

COMPARISON WITH T-BEAM TEST RESULTS

The paper by Mattock et al.[5] includes test results of T-beams reinforced with mild steel reinforcement in tension only to validate the derivation of the equivalent rectangular concrete stress distribution in ultimate strength design. The pertinent parameters of these test beams are shown in Table 3. Table 4 shows a comparison of the test results with the calculated capacities of LRFD, STD, and the nonlinear analysis.

In all cases where the depth to the neutral axis exceeds the depth of the top flange at nominal flexural strength, the ratio M_{test}/M_{calc} is unity or greater. The nonlinear analysis predicts the actual strength most accurately followed by STD and LRFD.

Ma et al.[22] tested NU1100 girders for negative moment, as if the girders were made continuous over an interior pier. The tension reinforcement was provided by mild steel reinforcement in the cast-in-place deck and, in the case of Specimen CB, high strength threaded rods projecting from the girder top flange. These tests were for a uniform concrete strength of 9130 psi (62.9 MPa) in the compression zone.

Castrodale et al.[23] tested composite T-beams with pretensioned strands. For both specimens, the concrete strength in the deck was significantly lower than that in the girder. The results of both series of tests, and the flexural capacity computed with the nonlinear analysis, are listed in Table 5. The nonlinear analysis conservatively predicts the flexural strength in all cases.

It is not possible to directly calculate the flexural strength of Specimen CB of Ma et al. with the approximate method of LRFD, since the section contains high strength steel rods. However, a strain compatibility analysis can be performed using the LRFD assumptions with respect to the equivalent rectangular stress block. Table 6 compares the pertinent parameters for Specimen CB using the nonlinear analysis and this LRFD approach. Fig. 21 shows the resulting compression zones. LRFD predicts a substantially greater depth to the neutral axis and about 9 percent less flexural capacity than the nonlinear analysis.

More importantly, the LRFD analysis results in an overreinforced section, while the nonlinear analysis does not. With the current limit of $c/d_e \le 0.42$, LRFD limits the calculated capacity of the section to about 89 percent of the nonlinear results. It is not clear what resistance factor ϕ should be used to determine the LRFD design strength in the current specifications.

The net tensile strain in the extreme tension steel at nominal flexural strength is calculated to be 0.0107 for the nonlinear analysis and 0.00369 for LRFD. The nonlinear analysis indicates a section that is well into the tension-controlled zone,

Table 5. Comparison with test results from Ma et al.[22] and Castrodale et al.[23]

	Specimen	c (in.)	$M_{nN\text{-}L}$ (kip-in.)	M_{test} (kip-in.)	$\frac{M_{test}}{M_{nN\text{-}L}}$
Ma et al.[22]	CB	10.51	91,308	99,768	1.09
	CC	7.97	76,764	79,500	1.04
Castrodale et al.[23]	1	7.00	3939	4626	1.17
	2	4.36	3293	3690	1.12

Note: 1 in. = 25.4 mm; 1 kip-in. = 0.113 kN-m.

Table 6. Comparison of Nonlinear and LRFD Analyses, Ma et al.[22] Specimen CB.

Parameter	Nonlinear	AASHTO LRFD
β_1	—	0.65
Neutral axis depth, c (in.)	10.51	21.41
Equivalent rectangular stress block, a (in.)	—	13.91
Stress in top reinforcing bar in deck, f_{s1} (ksi)	80.00	80.00
Stress in bottom reinforcing bar in deck, f_{s2} (ksi)	80.00	80.00
Stress in high strength rods, f_{sr} (ksi)	130.01	79.39
Effective depth to tension force, d_e (in.)	45.52	45.85
Calculated flexural strength, M_n (kip-in.)	91,308	83,724
Maximum reinforcement limit ($c/d_e \le 0.42$)	0.35 (OK)	0.47 (OVER)
Under-reinforced adjusted M_n (kip-in.)	91,308	81,456
Net tensile strain in extreme tension steel, ε_t	0.0107	0.00369
$\phi = 0.583 + 0.25\left(\frac{d_t}{c} - 1\right)$	1.00	0.89
ϕM_n (kip-in.)	91,308	74,562

Note: 1 in. = 25.4 mm; 1 ksi = 6.895 MPa; 1 kip-in. = 0.113 kN-m.

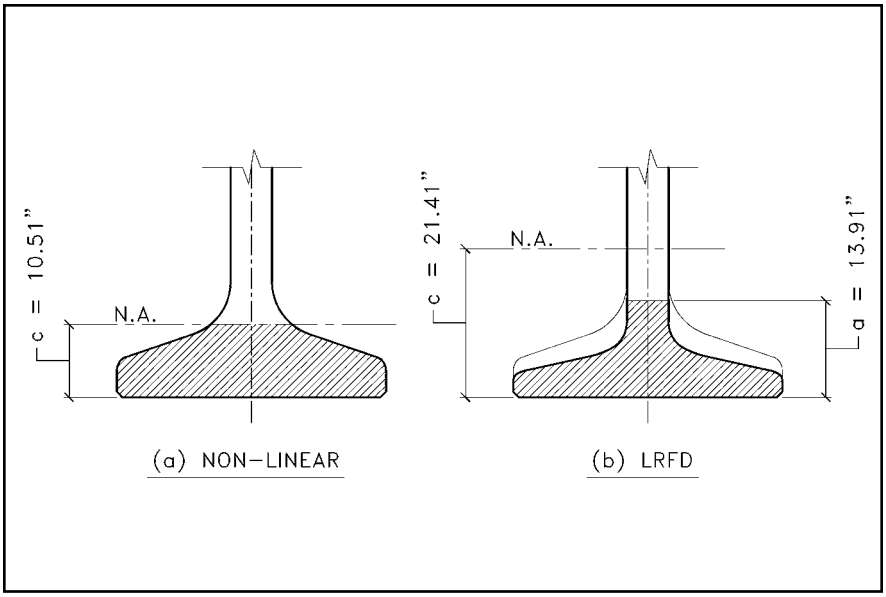

Fig. 21. Comparison of compression zones for Specimen CB (Ma et al.[22]) – Nonlinear analysis versus LRFD.

while LRFD indicates a section in the transition region. By applying a varying ϕ as proposed in this paper, LRFD would predict a design strength that is 82 percent of the design strength calculated with the nonlinear analysis and 75 percent of the experimental strength.

CONCLUSIONS

Based on the results of this study, the following conclusions can be drawn:

1. The equations for calculating the flexural strength of T-beams in the current AASHTO LRFD Specifications are not consistent with the original derivation of the equivalent rectangular concrete compressive stress distribution for flanged sections.

2. For non-prestressed T-beams of uniform strength, the equations given in the AASHTO Standard Specifications provide reasonable estimates of the flexural strength of flanged sections. This appears to be true for concrete strengths up to and including 15,000 psi (103 MPa).

3. For prestressed T-beams of uniform strength, a combination of the current AASHTO LRFD and Standard Specifications provides a reasonable approximation of flexural strength. In this case, the steel stress at nominal flexural strength is determined by the methods of LRFD, while the equivalent rectangular concrete compressive stress distribution of STD is used to calculate the depth to the neutral axis and flexural strength.

4. For T-beams with different concrete strengths in the flange and web, when the compressive stress block includes both types of concrete, the traditional equivalent rectangular concrete compressive stress distribution does not provide a reliable estimate of flexural strength.

5. The current AASHTO LRFD Specifications do not handle prestressed and non-prestressed flexural members in a consistent manner. Over-reinforced prestressed flexural members are allowed, while over-reinforced non-prestressed flexural members are not. No guidance is given for the determination of the resistance factor, ϕ, for over-reinforced prestressed members.

RECOMMENDATIONS

Based on the results of this study, the following recommendations are offered (see also Appendix C):

1. For prestressed and non-prestressed T-beams of uniform strength, the calculation methods of the Standard Specifications are recommended, with the exception that the LRFD method of calculating the stress in the prestressing steel at nominal flexural strength be retained. This is applicable to concrete strengths up to 15,000 psi (103 MPa). The more generalized PCI BDM analysis may also be used, and can include other contributors that may be present in the compression zone, such as the sloping portion of bridge girder flanges.

2. For prestressed and non-prestressed T-beams with different concrete strengths in the flange and web, it is conservative to use the proposed equations or the PCI BDM method assuming the T-beam to be of uniform strength at the lower of the concrete strengths in the flange and web. Otherwise, a nonlinear strain compatibility analysis of the type used in this study is recommended.

3. The authors recommend the elimination of maximum reinforcement limits and the adoption of a linearly varying ϕ in the AASHTO LRFD Specifications. This is a more rational approach that unifies the design of prestressed and non-prestressed flexural members, and also provides guidance for the value of the resistance factor in the transition zone between tension-controlled and compression-controlled members.

ACKNOWLEDGMENTS

The authors thank Dr. Maher Tadros and his students, and Dr. Reid Castrodale, for providing moral support and valuable information on the testing of T-beams at the University of Nebraska and the University of Texas at Austin, respectively.

The authors also thank the PCI JOURNAL reviewers for their valuable and constructive comments.

The opinions and conclusions expressed in this paper are those of the authors and are not necessarily those of the Washington State Department of Transportation.

REFERENCES

1. Seguirant, S. J., "Effective Compression Depth of T-Sections at Nominal Flexural Strength," Open Forum: Problems and Solutions, PCI JOURNAL, V. 47, No. 1, January-February 2002, pp. 100-105. See also discussion by A. E. Naaman and closure to discussion in V. 47, No. 3, May-June 2002, pp. 107-113.
2. Girgis, A., Sun, C., and Tadros, M. K., "Flexural Strength of Continuous Bridge Girders—Avoiding the Penalty in the AASHTO LRFD Specifications," Open Forum: Problems and Solutions, PCI JOURNAL, V. 47, No. 4, July-August 2002, pp. 138-141.
3. Naaman, A. E., "Rectangular Stress Block and T-Section Behavior," Open Forum: Problems and Solutions, PCI JOURNAL, V. 47, No. 5, September-October 2002, pp. 106-112.
4. AASHTO, *LRFD Bridge Design Specifications*, Third Edition, American Association of State Highway and Transportation Officials, Washington, DC, 2004.
5. Mattock, A. H., Kriz, L. B., and Hognestad, E., "Rectangular Concrete Stress Distribution in Ultimate Strength Design," *ACI Journal*, V. 32, No. 8, January 1961, pp. 875-928.
6. ACI Committee 318, "Commentary of Building Code Requirements for Reinforced Concrete (ACI 318R-83)," American Concrete Institute, Farmington Hills, MI, 1983.
7. Nawy, E. G., *Prestressed Concrete—A Fundamental Approach*, Second Edition, Prentice-Hall, Inc., Simon & Schuster / A Viacom Company, Upper Saddle River, NJ, 1996, pp. 187-189.
8. AASHTO, *Standard Specifications for Highway Bridges*, Seventeenth Edition, American Association of State Highway and Transportation Officials, Washington, DC, 2002.
9. *PCI Bridge Design Manual*, Precast/Prestressed Concrete Institute, Chicago, IL, 1997.
10. ACI Committee 318, "Building Code Requirements for Structural Concrete (ACI 318-02) and Commentary (ACI 318R-02)," American Concrete Institute, Farmington Hills, MI, 2002.
11. Collins, M. P., and Mitchell, D., *Prestressed Concrete Structures*, Prentice-Hall, Inc., A Division of Simon & Schuster, Englewood Cliffs, NJ, 1991, pp. 61-65.
12. Naaman, A. E., "Unified Design Recommendations for Reinforced, Prestressed, and Partially Prestressed Concrete Bending and Compression Members," *ACI Structural Journal*, V. 89, No. 2, March-April 1992, pp. 200-210.
13. Weigel, J. A., Seguirant, S. J., Brice, R., and Khaleghi, B., "High Performance Precast, Prestressed Concrete Girder Bridges in Washington State," PCI JOURNAL, V. 48, No. 2, March-April 2003, pp. 28-52.
14. ACI Committee 318, "Building Code Requirements for Structural Concrete (ACI 318-99) and Commentary (ACI 318R-99)," American Concrete Institute, Farmington Hills, MI, 1999.
15. Mast, R. F., "Unified Design Provisions for Reinforced and Prestressed Concrete Flexural and Compression Members," *ACI Structural Journal*, V. 89, No. 2, March-April 1992, pp. 185-199. See also discussions by R. K. Devalapura and M. K. Tadros, C. W. Dolan and J. V. Loscheider and closure to discussions in V. 89, No. 5, September-October 1992, pp. 591-593.
16. ACI Committee 318, "Building Code Requirements for Reinforced Concrete (ACI 318-89) and Commentary (ACI 318R-89)," American Concrete Institute, Farmington Hills, MI, 1989.
17. ACI Committee 318, "Building Code Requirements for Structural Concrete (ACI 318-95) and Commentary (ACI 318R-95)," American Concrete Institute, Farmington Hills, MI, 1995.
18. Bae, S., and Bayrak, O., "Stress Block Parameters for High Strength Concrete Members," *ACI Structural Journal*, V. 100, No. 5, September-October 2003, pp. 626-636.
19. Ibrahim, H. H. H., and MacGregor, J. G., "Tests of Eccentrically Loaded High-Strength Concrete Columns," *ACI Structural Journal*, V. 93, No. 5, September-October 1996, pp. 585-594.
20. Ozden, S., "Behavior of High-Strength Concrete Under Strain Gradient," MA Thesis, University of Toronto, Ontario, Canada, 1992, pp. 112-113.
21. Bayrak, O., "Seismic Performance of Rectilinearly Confined High-Strength Concrete Columns," PhD Dissertation, University of Toronto, Ontario, Canada, 1999, pp. 80-187.
22. Ma, Z., Huo, X., Tadros, M. K., and Baishya, M., "Restraint Moments in Precast/Prestressed Concrete Continuous Bridges," PCI JOURNAL, V. 43, No. 6, November-December 1998, pp. 40-57.
23. Castrodale, R. W., Burns, N. H., and Kreger, M. E., "A Study of Pretensioned High Strength Concrete Girders in Composite Highway Bridges—Laboratory Tests," Research Report 381-3, Center for Transportation Research, University of Texas at Austin, TX, January 1988.
24. Devalapura, R. K., and Tadros, M. K., "Critical Assessment of ACI 318 Eq. (18-3) for Prestressing Steel Stress at Ultimate Flexure," *ACI Structural Journal*, V. 89, No. 5, September-October 1992, pp. 538-546.
25. Naaman, A. E., "Limits of Reinforcement in 2002 ACI Code: Transition, Flaws, and Solution," *ACI Structural Journal*, V. 101, No. 2, March-April 2004, pp. 209-218.

APPENDIX A – NOTATION

a = depth of equivalent rectangular stress block, in.

A_c = area of portion of concrete compression block under consideration, sq in.

A_{ps} = area of prestressing steel, sq in.

A_s = area of non-prestressed tension reinforcement, sq in.

A_s' = area of compression reinforcement, sq in.

A_s^* = area of prestressing steel, sq in. (STD notation)

A_{sf} = area of tension reinforcement required to develop ultimate compressive strength of overhanging portions of flange, sq in. (STD notation)

A_{sr} = $A_s^* - A_{sf}$, sq in. (STD notation)

b = width of compression face of member, in.

b' = width of girder web, in. (STD notation)

b_w = width of girder web, in.

c = distance from extreme compression fiber to neutral axis, in.

C_{flange} = compression force in girder flange, kips

C_{web} = compression force in girder web, kips

d = distance from extreme compression fiber to centroid of prestressing force, in. (STD notation)

d_e = effective depth from extreme compression fiber to centroid of tensile force in tensile reinforcement, in.

d_t = distance from extreme compression fiber to extreme tension steel, in.

d_p = distance from extreme compression fiber to centroid of prestressing tendons, in.

d_s = distance from extreme compression fiber to centroid of non-prestressed tension reinforcement, in.

d_s' = distance from extreme compression fiber to centroid of compression reinforcement, in.

d_t = distance from extreme compression fiber to centroid of non-prestressed tension reinforcement, in. (STD notation)

E_c = modulus of elasticity of concrete, ksi

E_p = modulus of elasticity of prestressing steel, ksi

E_s = modulus of elasticity of reinforcing bars, ksi

f_c = average compressive stress in concrete slice for nonlinear analysis, ksi (Collins and Mitchell notation)[11]

f_c' = specified compressive strength of concrete at 28 days, unless another age is specified, psi

f_{pe} = effective stress in prestressing steel after losses, ksi

f_{pj} = stress in prestressing steel at jacking, ksi

f_{ps} = stress in prestressing steel at nominal flexural strength, ksi

f_{pu} = specified tensile strength of prestressing steel, ksi

f_{py} = yield strength of prestressing steel, ksi

f_{su}^* = stress in prestressing steel at nominal flexural strength, ksi (STD notation)

f_{sy} = yield stress of non-prestressed conventional reinforcement in tension, ksi (STD notation)

f_y = specified minimum yield stress of reinforcing bars, ksi

f_y' = specified minimum yield stress of compression reinforcement, ksi

h = overall depth of precast member, in.

H = overall depth of composite member, in.

h_f = structural deck slab thickness (not including wearing surface), in.

k = coefficient for type of tendon (LRFD notation)

k = factor to increase post-peak decay in stress for nonlinear concrete stress-strain curves (Collins and Mitchell notation)[11]

M_n = nominal flexural resistance, kip-in.

n = curve fitting factor for nonlinear concrete stress-strain curves (Collins and Mitchell notation)[11]

t = overall thickness of deck, in., or average thickness of flange of flanged member, in. (STD notation)

y_{flange} = distance from extreme compression fiber to resultant of compression force in flange, in.

y_{web} = distance from extreme compression fiber to resultant of compression force in web, in.

α_1 = stress intensity factor of equivalent rectangular compressive stress zone

β_1 = ratio of depth of equivalent uniformly stressed compression zone assumed in strength limit state to depth of actual compression zone

$\beta_{1(ave)}$ = area-weighted average value of β_1 for concretes of different strengths in the flange and web

ε_{cf} = strain in a concrete slice caused by f_c (Collins and Mitchell notation)[11]

ε_c' = strain when f_c reaches f_c' (Collins and Mitchell notation)[11]

ε_{ps} = tensile strain in layer of steel under consideration at nominal flexural strength

ε_t = net tensile strain in extreme tension steel at nominal strength

ϕ = resistance factor

ρ_m = maximum reinforcement ratio defined by $c/d_e = 0.42$

ρ_b = balanced reinforcement ratio where strain in extreme compressive fibers reaches 0.003 just as tension reinforcement reaches yield stress

APPENDIX B – FLEXURAL STRENGTH CALCULATIONS FOR COMPOSITE T-BEAMS

Find the flexural strength of a W83G girder made composite with a 7.50 in. (190 mm) thick cast-in-place deck, of which the top 0.50 in. (13 mm) is considered to be a sacrificial wearing surface. The girder spacing is 6.0 ft (1.83 m). Ignore the contribution of any non-prestressed reinforcing steel and the girder top flange. The girder configuration is shown in Fig. 16 with 70 – 0.6 in. (15.24 mm) diameter strands, and concrete strengths of 6000 psi (41.4 MPa) in the deck and 15,000 psi (103 MPa) in the girder.

Use the PCI Bridge Design Manual strain compatibility method using the average β_1 approximation. For comparison purposes, also use the PCI Bridge Design Manual strain compatibility method with β_1 for the girder concrete, and the nonlinear strain compatibility analysis.

Bare W83G Bridge Girder Data

Depth of girder	h = 82.68 in. (2100 mm)
Width of girder web	b_w = 6.10 in. (155 mm)
Area of prestressing steel	A_{ps} = 15.19 sq in. (9800 mm^2)
Specified tensile strength of prestressing steel	f_{pu} = 270.00 ksi (1862 MPa)
Initial jacking stress	f_{pj} = 202.50 ksi (1396 MPa)
Effective prestress after all losses	f_{pe} = 148.00 ksi (1020 MPa)
Modulus of elasticity of prestressing steel	E_p = 28,600 ksi (197200 MPa)
Design concrete strength	f'_c = 15,000 psi (103 MPa)

Composite W83G Bridge Girder Data

Overall composite section depth	H = 89.68 in. (2278 mm)
Deck slab width	b = 72.00 in. (1829 mm)
Deck slab thickness	t = 7.50 in. (190 mm)
Structural deck slab thickness	h_f = 7.00 in. (178 mm)
Depth to centroid of prestressing steel	d_p = 85.45 in. (2180 mm)
Design concrete strength	f'_c = 6000 psi (41.4 MPa)

Flexural Strength — PCI Bridge Design Manual (BDM) Strain Compatibility

For brevity, only the last iteration is shown. For a concrete strength of 15,000 psi (103 MPa), $\beta_1 = 0.65$.

Assume c = 30.75 in. (781 mm):

$$\varepsilon_{ps} = 0.003\left(\frac{d_p}{c} - 1\right) + \frac{f_{pe}}{E_p}$$
$$= 0.003\left(\frac{85.45}{30.75} - 1\right) + \frac{148.00}{28{,}600}$$
$$= 0.010511$$

Using the "power formula:"

$$f_{si} = \varepsilon_{ps}\left[887 + \frac{27{,}613}{\left(1 + (112.4\varepsilon_{ps})^{7.36}\right)^{1/7.36}}\right]$$
$$\le 270 \text{ ksi (1862 MPa)}$$

$$= (0.010511)\left[887 + \frac{27{,}613}{\left(1 + [112.4(0.010511)]^{7.36}\right)^{1/7.36}}\right]$$
$$= 246.56 \text{ ksi (1700 MPa)}$$

$$\sum A_{si}F_{si} = A_{ps}f_{si} = (15.19)(246.56)$$
$$= 3745 \text{ kips (16659 kN)}$$

Assume $\beta_{1(ave)} = 0.719$:

$$a = \beta_{1(ave)}\, c = (0.719)(30.75) = 22.10 \text{ in. (562 mm)}$$

$$\beta_{1(ave)} = \sum_j (f'_c A_c \beta_1)_j \Big/ \sum_j (f'_c A_c)_j$$
$$= \frac{(6)(7)(72)(0.75) + (15)(22.1 - 7)(6.10)(0.65)}{(6)(7)(72) + (15)(22.1 - 7)(6.10)}$$
$$= 0.719 \quad \textbf{OK}$$

$$\sum F_{cj} = 0.85f'_{c\,(deck)}\, h_f\, b + 0.85f'_{c\,(girder)}\,(a - h_f)\, b_w$$
$$= 0.85(6)(7)(72) + 0.85(15)(22.10 - 7)(6.10)$$
$$= 3745 \text{ kips (16659 kN)}$$
$$= 3745 \text{ kips (16659 kN)} \quad \textbf{OK}$$

The equivalent rectangular compressive stress distribution is shown in Fig. B1. Summing moments about the centroid of the prestressing steel:

$$M_n = 0.85f'_{c\,(deck)}\, h_f\, b\left(d_p - \frac{h_f}{2}\right)$$
$$+ 0.85f'_{c\,(girder)}\,(a - h_f)\, b_w\left(d_p - h_f - \frac{a - h_f}{2}\right)$$
$$= 0.85(6)(7)(72)\left(85.45 - \frac{7}{2}\right)$$
$$+ 0.85(15)(22.1 - 7)(6.10)\left(85.45 - 7 - \frac{22.1 - 7}{2}\right)$$
$$= 293{,}931 \text{ kip-in. (33213 kN-m)}$$

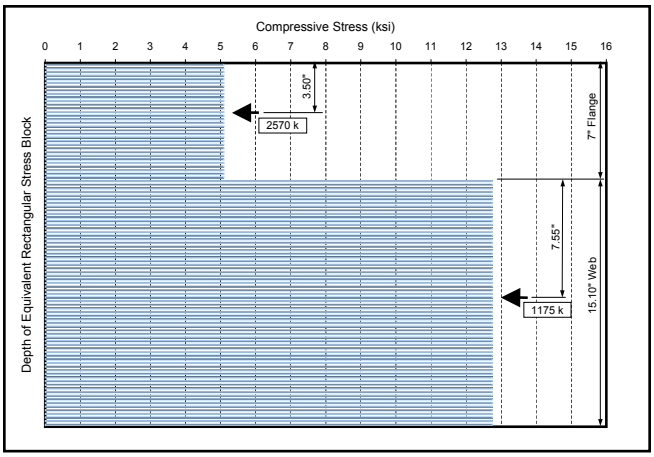

Fig. B1. Equivalent rectangular compressive stress distribution according to the PCI BDM analysis using $\beta_{1(ave)}$.

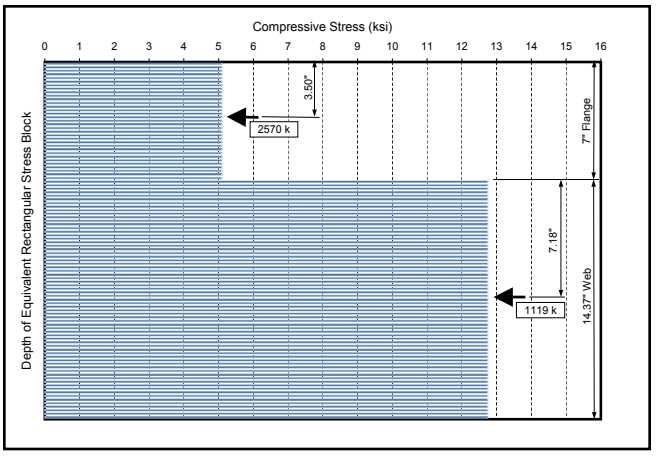

Fig. B2. Equivalent rectangular compressive stress distribution according to the PCI BDM analysis using β_1 of the deck concrete.

To calculate ϕ (note: the PCI BDM assumes $\phi = 0.70$ at $\varepsilon_t = 0.002$):

$$d_t = H - 2 = 89.68 - 2 = 87.68 \text{ in. (2225 mm)}$$

$$\phi = 0.5 + 0.3\left(\frac{d_t}{c} - 1\right)$$

$$= 0.5 + 0.3\left(\frac{87.68}{30.75} - 1\right) = 1.05 > 1.00 \quad \text{Use } 1.00$$

$$\phi M_n = 1.00(293{,}931)$$

$$= 293{,}931 \text{ kip-in. (33213 kN-m)}$$

Flexural Strength — PCI Bridge Design Manual with $\beta_1 = 0.65$

Assume $c = 32.87$ in. (835 mm)

$$\varepsilon_{ps} = 0.003\left(\frac{d_p}{c} - 1\right) + \frac{f_{pe}}{E_p}$$

$$= 0.003\left(\frac{85.45}{32.87} - 1\right) + \frac{148.00}{28{,}600}$$

$$= 0.009974$$

Using the "power formula:"

$$f_{si} = \varepsilon_{ps}\left[887 + \frac{27{,}613}{\left(1 + (112.4\varepsilon_{ps})^{7.36}\right)^{1/7.36}}\right]$$

$$\le 270 \text{ ksi (1862 MPa)}$$

$$= (0.009974)\left[887 + \frac{27{,}613}{\left(1 + [112.4(0.009974)]^{7.36}\right)^{1/7.36}}\right]$$

$$= 242.83 \text{ ksi (1674 MPa)}$$

$$\sum A_{si}F_{si} = A_{ps}f_{si} = (15.19)(242.83)$$
$$= 3689 \text{ kips (16408 kN)}$$

$$a = \beta_1 c = (0.65)(32.87) = 21.37 \text{ in. (543 mm)}$$

$$\sum F_{cj} = 0.85 f'_{c\,(deck)}\, h_f\, b + 0.85 f'_{c\,(girder)}\,(a - h_f)\, b_w$$

$$= 0.85(6)(7)(72) + 0.85(15)(21.37 - 7)(6.10)$$

$$= 3689 \text{ kips (16408 kN)}$$

$$= 3689 \text{ kips (16408 kN)} \quad \textbf{OK}$$

The equivalent rectangular compressive stress distribution is shown in Fig. B2.

$$M_n = 0.85 f'_{c\,(deck)}\, h_f b\left(d_p - \frac{h_f}{2}\right)$$
$$+ 0.85 f'_{c\,(girder)}\,(a - h_f)\, b_w\left(d_p - h_f - \frac{a - h_f}{2}\right)$$

$$= 0.85(6)(7)(72)\left(85.45 - \frac{7}{2}\right)$$

$$+ 0.85(15)(21.37 - 7)(6.10)\left(85.45 - 7 - \frac{21.37 - 7}{2}\right)$$

$$= 290{,}323 \text{ kip-in. (32805 kN-m)}$$

To calculate ϕ:

$$d_t = H - 2 = 89.68 - 2 = 87.68 \text{ in. (2225 mm)}$$

$$\phi = 0.5 + 0.3\left(\frac{d_t}{c} - 1\right)$$

$$= 0.5 + 0.3\left(\frac{87.68}{32.87} - 1\right) = 1.00 \quad \text{Use } 1.00$$

$$\phi M_n = 1.00(290{,}323)$$

$$= 290{,}323 \text{ kip-in. (32805 kN-m)}$$

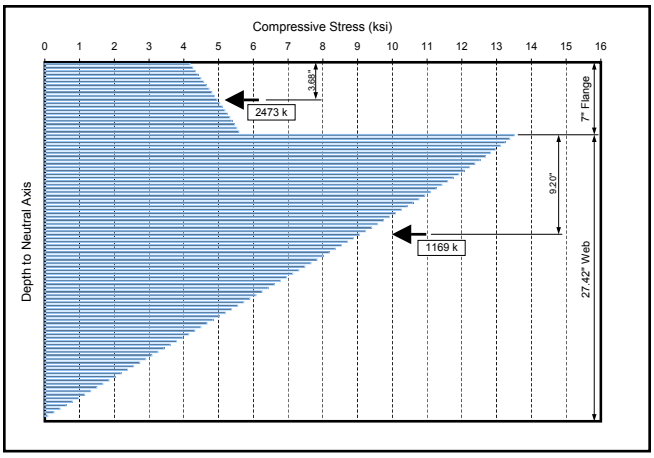

Fig. B3. Nonlinear compressive stress distribution.

Flexural Strength — Strain Compatibility with Nonlinear Concrete Stress Block

The concrete stress-strain curves for both the deck and girder concrete were taken from Collins and Mitchell[11] as shown in Fig. 5. The "power formula" of the PCI BDM was used to determine the stress in the prestressing steel for each iteration.

The concrete compression block was divided into 100 slices, 21 equal slices in the flange and 79 equal slices in the web for this case. The strain at the center of each slice was used to determine the average stress within that slice, which was multiplied by the area of the slice to determine the force in each slice.

The product of these forces and the distance to the center of each force from the top of the deck was used to calculate the resultant forces and eccentricities in the flange and web. Example calculations for the stresses in the slice at the top of the deck, and at the interface between the deck and girder, are as follows:

For the deck concrete:

$$E_c = \frac{(40{,}000\sqrt{f'_c} + 1{,}000{,}000)}{1000} = \frac{(40{,}000\sqrt{6000} + 1{,}000{,}000)}{1000}$$

$$= 4098 \text{ ksi } (28259 \text{ MPa})$$

$$n = 0.8 + \frac{f'_c}{2500} = 0.8 + \frac{6000}{2500} = 3.20$$

$$k = 0.67 + \frac{f'_c}{9000} = 0.67 + \frac{6000}{9000} = 1.337$$

$$\varepsilon'_c(1000) = \frac{f'_c}{E_c}\left(\frac{n}{n-1}\right) = \frac{6000}{4098}\left(\frac{3.2}{3.2-1}\right) = 2.129$$

For the top slice of deck:

$$y = \frac{7}{21(2)} = 0.167 \text{ in. } (4.2 \text{ mm})$$

$$\varepsilon_{cf} = \frac{0.003}{c}(c-y) = \frac{0.003}{34.42}(34.42 - 0.167) = 0.002985$$

$$f_c = (f'_c)\frac{n\left(\frac{\varepsilon_{cf}}{\varepsilon'_c}\right)}{n-1+\left(\frac{\varepsilon_{cf}}{\varepsilon'_c}\right)^{nk}} = (6)\frac{3.2\left(\frac{0.002985}{0.002129}\right)}{3.2-1+\left(\frac{0.002985}{0.002129}\right)^{3.2(1.337)}}$$

$$= 4.18 \text{ ksi } (28.8 \text{ MPa})$$

For the bottom slice of deck:

$$y = \frac{7}{21}(20) + \frac{7}{21(2)} = 6.833 \text{ in. } (174 \text{ mm})$$

$$\varepsilon_{cf} = \frac{0.003}{c}(c-y) = \frac{0.003}{34.42}(34.42 - 6.833) = 0.002404$$

$$f_c = (f'_c)\frac{n\left(\frac{\varepsilon_{cf}}{\varepsilon'_c}\right)}{n-1+\left(\frac{\varepsilon_{cf}}{\varepsilon'_c}\right)^{nk}} = (6)\frac{3.2\left(\frac{0.002404}{0.002129}\right)}{3.2-1+\left(\frac{0.002404}{0.002129}\right)^{3.2(1.337)}}$$

$$= 5.59 \text{ ksi } (38.5 \text{ MPa})$$

For girder concrete:

$$E_c = \frac{(40{,}000\sqrt{f'_c} + 1{,}000{,}000)}{1000} = \frac{(40{,}000\sqrt{15{,}000} + 1{,}000{,}000)}{1000}$$

$$= 5899 \text{ ksi } (40674 \text{ MPa})$$

$$n = 0.8 + \frac{f'_c}{2500} = 0.8 + \frac{15{,}000}{2500} = 6.80$$

$$k = 0.67 + \frac{f'_c}{9000} = 0.67 + \frac{15{,}000}{9000} = 2.337$$

$$\varepsilon'_c(1000) = \frac{f'_c}{E_c}\left(\frac{n}{n-1}\right) = \frac{15{,}000}{5899}\left(\frac{6.8}{6.8-1}\right) = 2.981$$

For the top slice of girder:

$$y = 7 + \frac{27.42}{79(2)} = 7.174 \text{ in. } (182 \text{ mm})$$

$$\varepsilon_{cf} = \frac{0.003}{c}(c-y) = \frac{0.003}{34.42}(34.42 - 7.174) = 0.002375$$

$$\text{Since } \frac{\varepsilon_{cf}}{\varepsilon_c'} = \frac{0.002375}{0.002981} = 0.797 < 1.0, \quad k = 1.0$$

$$f_c = (f_c')\frac{n\left(\frac{\varepsilon_{cf}}{\varepsilon_c'}\right)}{n - 1 + \left(\frac{\varepsilon_{cf}}{\varepsilon_c'}\right)^{nk}}$$

$$= (15)\frac{6.8\left(\frac{0.002375}{0.002981}\right)}{6.8 - 1 + \left(\frac{0.002375}{0.002981}\right)^{6.8(1.0)}}$$

$$= 13.51 \text{ ksi (93.2 MPa)}$$

The overall depth to the neutral axis was varied until the compressive force in the top equaled the tension force in the prestressing steel. Equilibrium was achieved at the nonlinear compressive stress distribution shown in Fig. B3. Summing moments about the centroid of the prestressing steel:

$$M_n = 2473(85.45 - 3.68) + 1169(85.45 - 7 - 9.20)$$
$$= 283{,}170 \text{ kip-in. (31997 MPa)}$$

To calculate ϕ:

$$d_t = H - 2 = 89.68 - 2 = 87.68 \text{ in. (2225 mm)}$$

$$\phi = 0.5 + 0.3\left(\frac{d_t}{c} - 1\right)$$
$$= 0.5 + 0.3\left(\frac{87.68}{34.42} - 1\right) = 0.96$$

$$\phi M_n = 0.96(283{,}170) = 273{,}034 \text{ kip-in. (30852 kN-m)}$$

A significant amount of additional capacity can be realized for this member by including the top flange of the W83G girder. The top flange is 49 in. (1245 mm) wide and approximately 6 in. (152 mm) deep. The large area and high strength of the top flange provide a considerable compressive contribution to the capacity analysis. The resulting depth to neutral axis, c, is 13.6 in. (345 mm) and the nominal capacity, ϕM_n, is 321,362 kip-in. (36295 kN-m). The resistance factor is 1.0. Accounting for the top flange results in 15 percent additional design strength.

APPENDIX C –
PROPOSED REVISIONS TO AASHTO LRFD, THIRD EDITION, 2004

Item No. 1

Add the following definitions to Article 5.2:

Compression-controlled section – A cross section in which the net tensile strain in the extreme tension steel at nominal strength is less than or equal to the compression-controlled strain limit.

Compression-controlled strain limit – The net tensile strain at balanced strain conditions.

Extreme tension steel – The reinforcement (prestressed or non-prestressed) that is farthest from the extreme compression fiber.

Net tensile strain – The tensile strain at nominal strength exclusive of strains due to effective prestress, creep, shrinkage and temperature.

Tension-controlled section – A cross section in which the net tensile strain in the extreme tension steel at nominal strength is greater than or equal to 0.005.

Item No. 2

Add the following to Article 5.3:

d_t = distance from extreme compression fiber to centroid of extreme tension steel (IN) (C5.5.4.2.1, C5.7.2.1)

ε_t = net tensile strain in extreme tension steel at nominal strength (C5.5.4.2.1, C5.7.2.1)

Delete the following from Article 5.3:

~~A_{cc} = area of concrete element in compression of corresponding strength (5.7.2.2)~~

Item No. 3

Revise Article 5.5.4.2.1 as follows:

1.1.1.1.1 Conventional Construction

Resistance factor ϕ shall be taken as:

- For ~~flexure and tension of~~ tension-controlled reinforced concrete sections as defined in Article 5.7.2.1 ..... 0.90
- For ~~flexure and tension of~~ tension-controlled prestressed concrete sections as defined in Article 5.7.2.1 ..... 1.00
- For shear and torsion:
  - normal weight concrete 0.90
  - lightweight concrete 0.70
- For ~~axial~~ compression-controlled sections with spirals or ties, as defined in Article 5.7.2.1, except as specified in Article 5.10.11.4.1b for Seismic Zones 3 and 4 at the extreme event limit state 0.75

The balance of the bulleted items remains unchanged.

~~For compression members with flexure, the value of ϕ may be increased linearly to the value for flexure as the factored axial load resistance, ϕP_n, decreases from $0.10 f'_c A_g$ to 0.~~

For sections in which the net tensile strain in the extreme tension steel at nominal strength is between the limits for compression-controlled and tension-controlled sections, ϕ may be linearly increased from 0.75 to that for tension-controlled sections as the net tensile strain in the extreme tension steel increases from the compression-controlled strain limit to 0.005.

For tension-controlled partially prestressed components ~~in flexure with or without tension~~, the value of ϕ may be taken as:

The balance of the Article remains unchanged.

Item No. 4

Add the following to Article C5.5.4.2.1 prior to the existing text:

In applying the resistance factors for tension-controlled and compression-controlled sections, the axial tensions and compressions to be considered are those caused by external forces. Effects of prestressing forces are not included.

In editions of and interims to the LRFD specifications prior to 2005, the provisions specified the magnitude of the resistance factor for cases of axial load or flexure, or both, in terms of the type of loading. For these cases, the ϕ-factor is now determined by the strain conditions at a cross section, at nominal strength. The background and basis for these provisions are given in Mast (1992) and ACI 318-02.

A lower ϕ-factor is used for compression-controlled sections than is used for tension-controlled sections because compression-controlled sections have less ductility, are more sensitive to variations in concrete strength, and generally occur in members that support larger loaded areas than members with tension-controlled sections.

For sections subjected to axial load with flexure, factored resistances are determined by multiplying both $\boldsymbol{P_n}$ and $\boldsymbol{M_n}$ by the appropriate single value of ϕ. Compression-controlled and tension-controlled sections are defined in Article 5.7.2.1 as those that have net tensile strain in the extreme tension steel at nominal strength less than or equal to the compression-controlled strain limit, and equal to or greater than 0.005, respectively. For sections with net tensile strain ε_t in the extreme tension steel at nominal strength between the above limits, the value of ϕ may be determined by linear interpolation, as shown in Figure C5.5.4.2.1-1. The concept of net tensile strain ε_t is discussed in Article C5.7.2.1. Classifying sections as tension-controlled, transition or compression-controlled, and linearly varying the resistance factor in the transition zone between reasonable values for the two extremes, provides a rational approach for determining ϕ and limiting the capacity of over-reinforced sections.

The balance of the existing text remains unchanged.

Item No. 5

Add bulleted items to the end of the list of Article 5.7.2.1 as follows:

- Balanced strain conditions exist at a cross section when tension reinforcement reaches the strain corresponding to its specified yield strength f_y just as the concrete in compression reaches its assumed ultimate strain of 0.003.
- Sections are compression-controlled when the net tensile strain in the extreme tension steel is equal to or less than the compression-controlled strain limit at the time the concrete in compression reaches its assumed strain limit of 0.003. The compression-controlled strain limit is the net tensile strain in the reinforcement at balanced strain conditions. For Grade 60 reinforcement, and for all prestressed reinforcement, the compression-controlled strain limit may be set equal to 0.002.
- Sections are tension-controlled when the net tensile strain in the extreme tension steel is equal to or greater than 0.005 just as the concrete in compression reaches its assumed strain limit of 0.003. Sections with net tensile strain in the extreme tension steel between the compression-controlled strain limit and 0.005 constitute a transition region between compression-controlled and tension-controlled sections.
- The use of compression reinforcement in conjunction with additional tension reinforcement is permitted to increase the strength of flexural members.

Item No. 6

Add commentary to Article C5.7.2.1 to accompany the bulleted items of Item No. 5 as follows:

The nominal flexural strength of a member is reached when the strain in the extreme compression fiber reaches the assumed strain limit of 0.003. The net tensile strain ε_t is the tensile strain in the extreme tension steel at nominal strength, exclusive of strains due to prestress, creep, shrinkage and temperature. The net tensile strain in the extreme tension steel is determined from a linear strain distribution at nominal strength, as shown in Figure C5.7.2.1-1, using similar triangles.

When the net tensile strain in the extreme tension steel is sufficiently large (equal to or greater than 0.005), the section is defined as tension-controlled where ample warning of failure with excessive deflection and cracking may be expected. When the net tensile strain in the extreme tension steel is small (less than or equal to the compression-controlled strain limit), a brittle failure condition may be expected, with little warning of impending failure. Flexural members are usually tension-controlled, while compression members are usually compression-controlled. Some sections, such as those with small axial load and large bending moment, will have net tensile strain in the extreme tension steel between the above limits. These sections are in a transition region between compression- and tension-controlled sections. Article 5.5.4.2.1 specifies the appropriate resistance factors for tension-controlled and compression-controlled sections, and for intermediate cases in the transition region.

Before the development of these provisions, the limiting tensile strain for flexural members was not stated, but was implicit in the maximum reinforcement limit that was given as $c/d_t \le 0.42$, which corresponded to a net tensile strain at the centroid of the tension reinforcement of 0.00414. The net

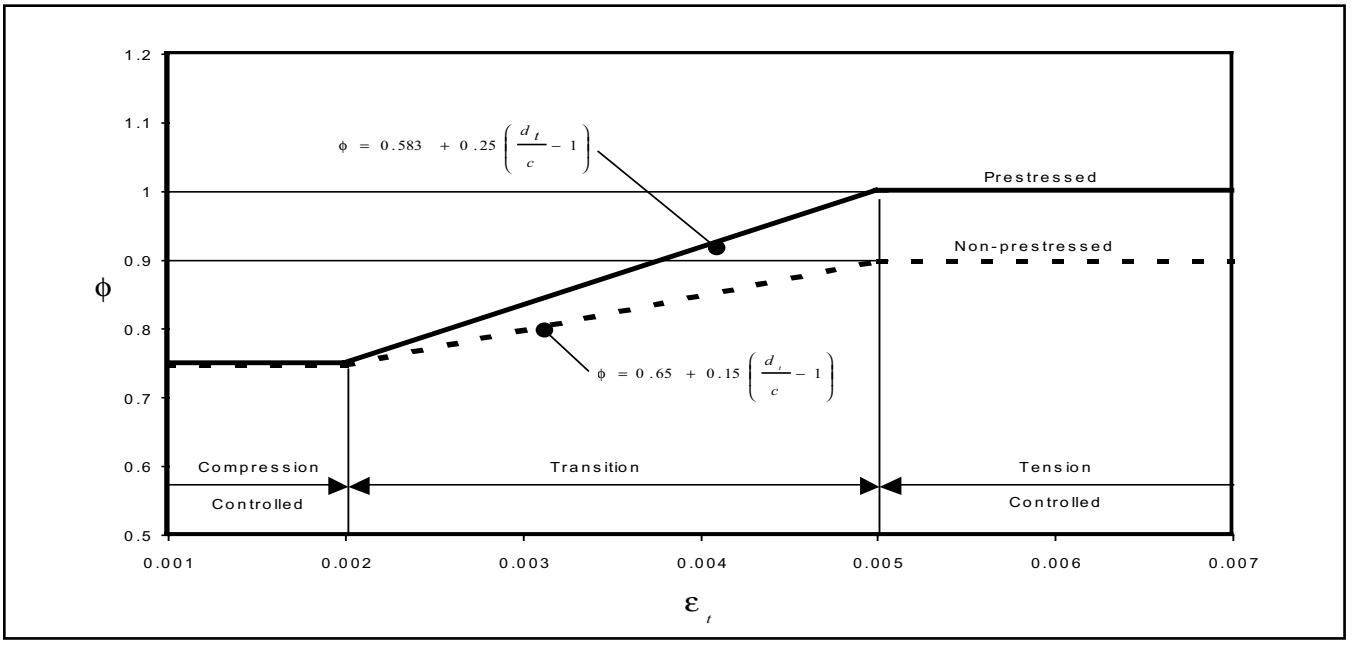

Figure C5.5.4.2.1-1 – Variation of ϕ with net tensile strain ε_t and d_t/c for Grade 60 reinforcement and for prestressing steel.

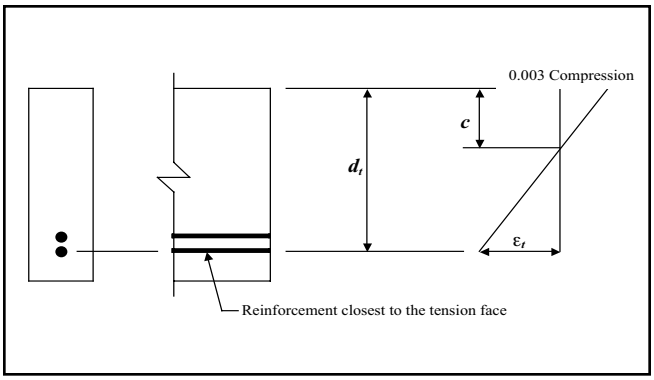

Figure C5.7.2.1-1 – Strain distribution and net tensile strain.

tensile strain limit of 0.005 for tension-controlled sections was chosen to be a single value that applies to all types of steel (prestressed and nonprestressed) permitted by this specification.

Unless unusual amounts of ductility are required, the 0.005 limit will provide ductile behavior for most designs. One condition where greater ductile behavior is required is in design for redistribution of moments in continuous members and frames. Article 5.7.3.5 permits redistribution of negative moments. Since moment redistribution is dependent on adequate ductility in hinge regions, moment redistribution is limited to sections that have a net tensile strain of at least 0.0075.

For beams with compression reinforcement, or T-beams, the effects of compression reinforcement and flanges are automatically accounted for in the computation of net tensile strain ε_t.

Item No. 7

Delete the second paragraph of Article 5.7.2.2 as shown:

~~In composite construction, the stress block factor, β_1, may be different for concrete strengths in the compression block. In this case the actual values of β_1 or alternatively an average value of β_1 may be assumed as follows:~~

$$\beta_{1(ave)} = \frac{\sum(f'_c A_{cc} \beta_1)}{\sum(f'_c A_{cc})}$$

~~where:~~

~~A_{cc} = area of concrete element in compression of corresponding strength~~

The balance of the Article remains unchanged.

Item No. 8

Delete the last paragraph of Article C5.7.2.2 and replace with the following:

~~The designer may utilize β_1 of the slab for composite designs.~~ For sections that consist of a beam with a composite slab of different concrete strength, and the compression block includes both types of concrete, it is conservative to assume the composite beam to be of uniform strength at the lower of the concrete strengths in the flange and web. If a more refined estimate of concrete strength is warranted, a more rigorous analysis method should be used. Examples of such analytical techniques are presented in Weigel, Seguirant, Brice and Khaleghi (2003) and Seguirant, Brice and Khaleghi (2005).

Item No. 9

Replace Equation 5.7.3.1.1-3 with the equation shown below:

$$c = \frac{A_{ps} f_{pu} + A_s f_y - A'_s f'_y - 0.85 f'_c (b - b_w) h_f}{0.85 f'_c b_w \beta_1 + k A_{ps} \frac{f_{pu}}{d_p}} \qquad (5.7.3.1.1\text{-}3)$$

Replace Equation 5.7.3.1.2-3 with the equation shown below:

$$c = \frac{A_{ps} f_{pu} + A_s f_y - A'_s f'_y - 0.85 f'_c (b - b_w) h_f}{0.85 f'_c b_w \beta_1} \qquad (5.7.3.1.2\text{-}3)$$

Item No. 10

Revise Article 5.7.3.2.2 as follows and replace Equation 5.7.3.2.2-1 with the equation shown below:

For flanged sections subjected to flexure about one axis and for biaxial flexure with axial load as specified in Article 5.7.4.5, where the approximate stress distribution specified in Article 5.7.2.2 is used ~~and the tendons are bonded~~ and where the compression flange depth is less than ~~c~~ $a = \beta_1 c$, as determined in accordance with Equations 5.7.3.1.1-3, 5.7.3.1.1-4, 5.7.3.1.2-3 or 5.7.3.1.2-4, the nominal flexural resistance may be taken as:

$$M_n = A_{ps} f_{ps} \left(d_p - \frac{a}{2} \right) + A_s f_y \left(d_s - \frac{a}{2} \right) - A'_s f'_y \left(d'_s - \frac{a}{2} \right) + 0.85 f'_c (b - b_w) h_f \left(\frac{a}{2} - \frac{h_f}{2} \right) \qquad (5.7.3.2.2\text{-}1)$$

Also delete β_1 *from the list of definitions following Equation 5.7.3.2.2-1.*

Item No. 11

Delete current Article C5.7.3.2.2 in its entirety, including Figure C5.7.3.2.2-1, and replace with:

In previous editions and interims of the LRFD Specifications, the factor β_1 was applied to the flange overhang term of Equations 1, 5.7.3.1.1-3 and 5.7.3.1.2-3. This was not consistent with the original derivation of the equivalent rectangular stress block as it applies to flanged sections (Mattock, Kriz and Hognestad 1961). For the current LRFD Specification, the β_1 factor has been removed from the flange overhang term of these equations. See also Seguirant (2002), Girgis, Sun and Tadros (2002), Naaman (2002), Weigel, Seguirant, Brice and Khaleghi (2003), Baran, Schultz and French (2005), and Seguirant, Brice and Khaleghi (2005).

Item No. 12

Revise Article 5.7.3.2.3 as follows:

For rectangular sections subjected to flexure about one axis and for biaxial flexure with axial load as specified in Article 5.7.4.5, where the approximate stress distribution specified in Article 5.7.2.2 is used and where the compression flange depth is not less than ~~$\boldsymbol{c}$~~ $\boldsymbol{a} = \beta_1 \boldsymbol{c}$ as determined in accordance with Equations 5.7.3.1.1-~~3~~4 or 5.7.3.1.2-4, the nominal flexural resistance $\boldsymbol{M_n}$ may be determined by using Equations 5.7.3.1.1-1 through 5.7.3.2.2-1, in which case $\boldsymbol{b_w}$ shall be taken as $\boldsymbol{b}$.

Item No. 13

Revise the first paragraph of Article 5.7.3.2.5 as follows:

Alternatively, the strain compatibility approach may be used~~, in lieu of the rectangular stress distribution, specified in Article 5.7.2.2,~~ if more precise calculations are required. ~~Other~~ The appropriate provisions of Article 5.7.2.1 shall apply.

The balance of the Article remains unchanged.

Item No. 14

Remove all of Article 5.7.3.3.1 and replace with
[PROVISION DELETED IN 2005]

Item No. 15

Remove all of Article C5.7.3.3.1 and replace with:

In editions of and interims to the LRFD specifications prior to 2005, Article 5.7.3.3.1 limited the tension reinforcement quantity to a maximum amount such that the ratio $\boldsymbol{c/d_e}$ did not exceed 0.42. Sections with $\boldsymbol{c/d_e} > 0.42$ were considered over-reinforced. Over-reinforced nonprestressed members were not allowed, whereas prestressed and partially prestressed members with PPR greater than 50 percent were if "it is shown by analysis and experimentation that sufficient ductility of the structure can be achieved." No guidance was given for what "sufficient ductility" should be, and it was not clear what value of ϕ should be used for such over-reinforced members.

The current provisions of LRFD eliminate this limit and unify the design of prestressed and nonprestressed tension- and compression-controlled members. The background and basis for these provisions are given in Mast (1992). Below a net tensile strain in the extreme tension steel of 0.005, as the tension reinforcement quantity increases, the factored resistance of prestressed and non-prestressed sections is reduced in accordance with Article 5.5.4.2.1. This reduction compensates for decreasing ductility with increasing over-strength. Only the addition of compression reinforcement in conjunction with additional tension reinforcement can result in an increase in the factored flexural resistance of the section.

Item No. 16

Revise Article 5.7.3.5 as follows:

In lieu of more refined analysis, where bonded reinforcement that satisfies the provisions of Article 5.11 is provided at the internal supports of continuous reinforced concrete beams ~~and where the $\boldsymbol{c/d_e}$ ratio does not exceed 0.28~~, negative moments determined by elastic theory at strength limit states may be increased or decreased by not more than ~~the following percentage:~~ 1000 ε_t percent, with a maximum of 20 percent. Redistribution of negative moments shall be made only when ε_t is equal to or greater than 0.0075 at the section at which moment is reduced.

~~$$20\left(1 - 2.36\frac{c}{d_e}\right) \qquad (5.7.3.5\text{-}1)$$~~

The balance of the Article remains unchanged.

Item No. 17

Add new Article C5.7.3.5 as follows:

In editions of and interims to the LRFD specifications prior to 2005, Article 5.7.3.5 specified the permissible redistribution percentage in terms of the $\boldsymbol{c/d_e}$ ratio. The current specification specifies the permissible redistribution percentage in terms of net tensile strain ε_t. The background and basis for these provisions are given in Mast (1992).

Item No. 18

Add References 1, 2, 3, 5, 10, 13, and 15 of this paper to LRFD, as well as a reference to this paper. Also add the following reference:

Baran, E., Schultz, A. E., and French, C. E., "Analysis of the Flexural Strength of Prestressed Concrete Flanged Sections," PCI JOURNAL, V. 50, No. 1, January-February 2005, pp. 74-93.

APPENDIX D –
DERIVATION OF EQ. (10) FROM STD EQ. 9-14a [EQ. (11)]

Substituting LRFD notation where possible and deleting ϕ, Eq. (11) becomes:

$$M_n = A_{sr} f_{ps}\, d_p \left(1 - 0.6\,\frac{A_{sr} f_{ps}}{b_w d_p f'_c}\right) + A_s f_y\,(d_s - d_p) + 0.85 f'_c\,(b - b_w)\,h_f \left(d_p - \frac{h_f}{2}\right) \tag{D-1}$$

$$A_{sr} = A_{ps} + \frac{A_s f_y}{f_{ps}} - \frac{0.85 f'_c\,(b - b_w)\,h_f}{f_{ps}} \tag{D-2}$$

First, by substituting Eq. (D-2) into Eq. (D-1), and 1/2(0.85) for 0.6:

$$d_p \left[1 - \left(\frac{1}{2(0.85)}\right) \frac{\left(A_{ps} + \frac{A_s f_y}{f_{ps}} - \frac{0.85 f'_c\,(b - b_w)\,h_f}{f_{ps}}\right) f_{ps}}{b_w d_p f'_c}\right]$$

$$= \left(d_p - \frac{A_{ps} f_{ps} + A_s f_y - 0.85 f'_c\,(b - b_w)\,h_f}{2(0.85) f'_c\, b_w}\right) = \left(d_p - \frac{a}{2}\right)$$

Then:

$$M_n = A_{sr} f_{ps} \left(d_p - \frac{a}{2}\right) + A_s f_y\,(d_s - d_p) + 0.85 f'_c\,(b - b_w)\,h_f \left(d_p - \frac{h_f}{2}\right)$$

Again, substituting for A_{sr}:

$$M_n = \left(A_{ps} + \frac{A_s f_y}{f_{ps}} - \frac{0.85 f'_c\,(b - b_w)\,h_f}{f_{ps}}\right) f_{ps} \left(d_p - \frac{a}{2}\right) + A_s f_y\,(d_s - d_p) + 0.85 f'_c\,(b - b_w)\,h_f \left(d_p - \frac{h_f}{2}\right)$$

$$= A_{ps} f_{ps} \left(d_p - \frac{a}{2}\right) + A_s f_y \left(d_p - \frac{a}{2}\right) - 0.85 f'_c\,(b - b_w)\,h_f \left(d_p - \frac{a}{2}\right) + A_s f_y\,(d_s - d_p) + 0.85 f'_c\,(b - b_w)\,h_f \left(d_p - \frac{h_f}{2}\right)$$

$$= A_{ps} f_{ps} \left(d_p - \frac{a}{2}\right) + A_s f_y \left(d_p - \frac{a}{2} + d_s - d_p\right) + 0.85 f'_c\,(b - b_w)\,h_f \left(d_p - \frac{h_f}{2} - d_p + \frac{a}{2}\right)$$

$$M_n = A_{ps} f_{ps} \left(d_p - \frac{a}{2}\right) + A_s f_y \left(d_s - \frac{a}{2}\right) + 0.85 f'_c\,(b - b_w)\,h_f \left(\frac{a}{2} - \frac{h_f}{2}\right) \tag{D-3}$$

Eq. (D-3) is the same as Eq. (10), except that Eq. (D-3) is missing the term representing mild steel compression reinforcement. Therefore, although it is used in this paper in a different form, Eq. (10) is the same as STD Eq. 9-14a [Eq. (11) of this paper].